AD-A112 545 NAVAL RESEARCH LAB WASHINGTON DC F/G 20/5
APPLICATION OF TIME-RESOLVED SPECTROSCOPIES TO THE STUDY OF ENE--ETC(U)
MAR 82 J M SCHNUR
UNCLASSIFIED NRL-MR-4755 NL

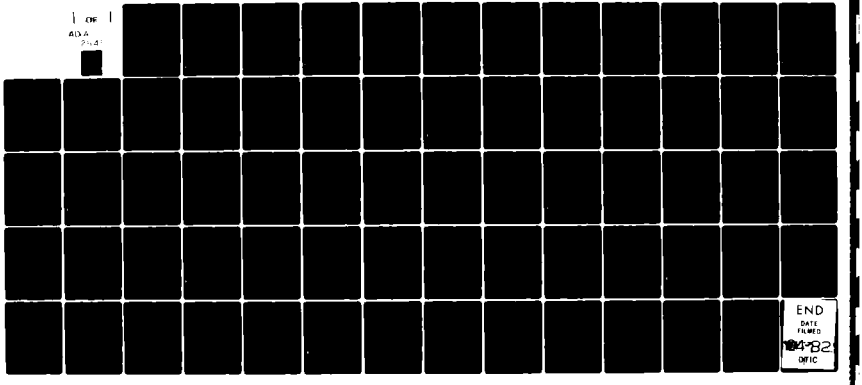

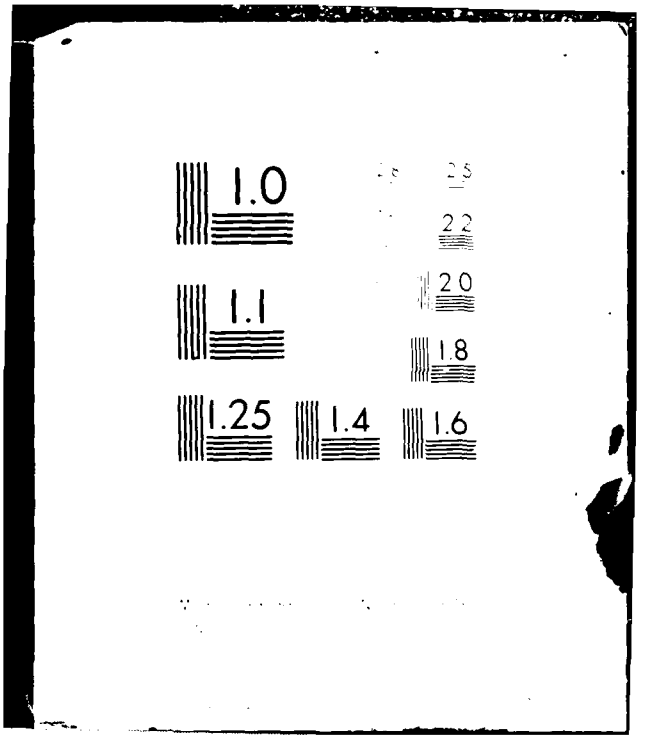
1.0
1.1
1.25
1.4
1.6
2.2
2.0
1.8

(2)

NRL Memorandum Report 4755

Application of Time-Resolved Spectroscopies to the Study of Energetic Materials — 1981

A Summary Report

J. M. SCHNUR

Optical Probes Branch
Optical Sciences Division

March 5, 1982

This research was supported in part by the Office of Naval Research.

NAVAL RESEARCH LABORATORY
Washington, D.C.

Approved for public release; distribution unlimited.

REPORT DOCUMENTATION PAGE

1 REPORT NUMBER: NRL Memorandum Report 4755	2 GOVT ACCESSION NO. AD-A112 545
4 TITLE (and Subtitle): APPLICATION OF TIME-RESOLVED SPECTROSCOPIES TO THE STUDY OF ENERGETIC MATERIALS — 1981	5 TYPE OF REPORT & PERIOD COVERED: Interim report on a continuing NRL problem.
	6 PERFORMING ORG. REPORT NUMBER
7 AUTHOR(s): J.M. Schnur	8 CONTRACT OR GRANT NUMBER(s)
9 PERFORMING ORGANIZATION NAME AND ADDRESS: Naval Research Laboratory, Washington, DC 20375	10 PROGRAM ELEMENT, PROJECT, TASK AREA & WORK UNIT NUMBERS: RR-021-02-02; ONR; 65-1192-0-2; 65-1200-0-2; 65-1194-0-2
11 CONTROLLING OFFICE NAME AND ADDRESS	12 REPORT DATE: March 5, 1982
	13 NUMBER OF PAGES: 66
14 MONITORING AGENCY NAME & ADDRESS (if different from Controlling Office)	15 SECURITY CLASS. (of this report): UNCLASSIFIED
	15a DECLASSIFICATION/DOWNGRADING SCHEDULE

16 DISTRIBUTION STATEMENT (of this Report)

Approved for public release; distribution unlimited.

17 DISTRIBUTION STATEMENT (of the abstract entered in Block 20, if different from Report)

18 SUPPLEMENTARY NOTES

This research was supported in part by the Office of Naval Research and the Naval Research Laboratory.

19 KEY WORDS (Continue on reverse side if necessary and identify by block number)

Picosecond	Propellent binders
Energetic materials	Fast reactions
Lasers	Spectroscopy

20 ABSTRACT (Continue on reverse side if necessary and identify by block number)

This report contains a detailed description (including 4 manuscripts) of the research performed as a result of the ONR, and NRL research program (NRL 65-1192).

DD FORM 1 JAN 73 1473 EDITION OF 1 NOV 65 IS OBSOLETE

SECURITY CLASSIFICATION OF THIS PAGE (When Data Entered)

CONTENTS

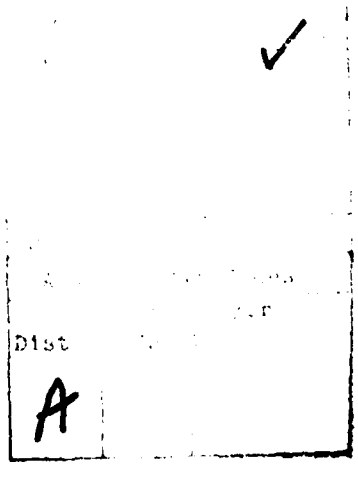

Application of Time-Resolved Laser Spectroscopies to the Study of Energetic Materials - 1981

Summary Report

I. Introduction

This report describes recent progress in NRL's research involving the application of advanced spectroscopies to the study of energetic materials. This program is currently jointly funded by the Office of Naval Research and the Naval Research Laboratory as part of their collaborative Special Focus Program in the area of energetic materials.

The goal of this initial spectroscopic studies are to provide the appropriate species identification protocols suitable for the study of fast energetic reactions stimulated by light, heat, and/or shock.

One of the major objectives of this Special Focus Program is to identify and characterize the important initial stages of energetic reactions as a function of initiation mode. In order to do this, techniques must be developed to observe the critical chemical fragments in the required time scales [e.g. 10^{-11} sec] and to elucidate the kinetics. Using these data attempts will be made to modify and control the course of the observed energetic reactions.

The initial species identification experiments have been performed in the Short Pulse Section of the Optical Probes Branch [Code 6510] at NRL. Collaboration with the Chemistry Departments of Georgetown University, Johns Hopkins University and Washington State University, have been quite useful to the program during the past year.

II. Progress FY 81

The time definition inherent in picosecond pulse excitation enables the near-instantaneous deposition of energy into the molecular system before secondary reactions or collisions can occur. As a consequence of the high optical flux densities obtainable from our short pulse lasers, we can readily excite molecular systems through either single or multiphoton absorption processes.

Unimolecular processes are of interest in regard to the determination of primary photo-induced events. There are many questions about unimolecular photodissociation which are likely to be answered through the application of recently developed short pulse techniques. For isolation of specifically

Manuscript submitted December 17, 1981.

unimolecular and early collisional processes, we have been performing experiments on a variety of simple gas-phase organic molecules. (Table I)

Table I

GASES	EMISSIVE SPECIES/STATES	
CH_3NO_2	C_2	$d^3\Pi_g \rightarrow a^3\Pi_u$; $C^1\Pi_g \rightarrow A^1\Pi_u$
C_2H_2	CN	$B^2\Sigma^+ \rightarrow X^2\Sigma^+$
CH_3CN	CH	$A^2\Delta \rightarrow X^2\Pi$
CH_2CO	H_α, H_β	Balmer Series
CO	C	$3^1P^o \rightarrow 2^1S$
CH_4	C^+	$3^2P^o \rightarrow 2^2S$
HCN	O	$3^5P \rightarrow 3^5S$; $3^3P \rightarrow 3^3S$

A. Acetylene

Extensive data have been collected for short pulse uv photolysis (25 ps, 266 nm, 10 mJ) of C_2H_2. The dominant emissive fragment product is the carbon diradical, C_2 $d^3\Pi_g$, and its consequent Swan emission ($d^3\Pi_g \rightarrow a^3\Pi_u$). The characteristic approaches which we have developed fix upon individual species isolated spectroscopically and detected in emission. Our results have given conclusive evidence that the lowest order process yielding emissive C_2^* is unimolecular and occurs in less than a nanosecond. Streak camera data indicate a grow-in time for this fragment of about 200 picoseconds. The unimolecular nature of the process was confirmed by performing isotopic labeling experiments utilizing mixtures of $^{12}C_2H_2$ and $^{13}C_2H_2$. Emission characteristic of the collisionally produced fragment $(^{12}C\ ^{13}C)^*$ was sought, but very little signal attributable to this species was observed at early times of less than a few nanoseconds. After several nanoseconds, a grow in of the $(^{12}C\ ^{13}C)^*$ fragment was detected.

Thus C_2^* also is produced intermolecularly from fragments of acetylene in secondary processes that are exhausted within several nanoseconds (~ 7ns at 5 torr). This development must be regarded as fast on the scale of collision rates, although it is readily observed by our instrumentation. The collision partners in this C_2^* formation process appear to be pairs of excited CH^* radicals. Emission spectra from CH $A^2\Delta$ have been observed. These spectra exhibit parent quenching with $k_Q \sim 3 \times 10^{-10}$ sec^{-1}, which is typical for radicals and/or excited electronic states. (Normal molecules give substantially lower rates.) Employing the hypothesis of a collisional formation rate proportional to $(CH^*)^2$ and considering known C_2^* decay rates, the CH^* emission time profiles indicate that these are pertinent rates of precursor exhaustion.

B. Carbon Monoxide

C_2 $d^3\Pi_g$ is also formed upon the irradiation of CO with intense picosecond pulses at 266 nm. The processes involved in the formation of C_2 from CO are clearly different from those for other molecules studies, e.g. acetylene, acetonitrile, ketene, methane, etc. There is in fact an extensive literature on related observations of C_2 Swan emission from CO parents. The anomalous features in the emission spectrum, first reported by Fowler some 70 years ago, have attracted repeated spectroscopic and kinetic studies. There has, however, been a deficiency in temporal studies, probably due to lack of instrumental capability.

The most striking feature that is observed is a strong relative enhancement of $V' = 6$ in the Swan spectrum. This is not quite unique to CO, having been also observed in CH_4 and flames. Our time resolved studies reveal that Swan excitation occurs through distinct early and late processes. However, even the early process produces emission protracted far beyond the radiation lieftime of 120 ns. The late process endures for over 20 μs and is not affected by pressure. In addition, we have demonstrated that it is the late process which is exclusively responsible for the $V' = 6$ enhancement; the early process yields a vibrational distribution typical of the other parent species listed above.

Our results are consistant with a hypothesis that resonant curve crossing within C_2^* is responsible for $V' = 6$ enhancement; indeed a single-triplet transfer $I^1\Delta_g \rightarrow d^3\Pi_g$ may even account for 20 μs delays. Protracted chemiluminescence from such a simple parent as CO is quite unusual and was not expected.

C. Acetonitrile

The temporal profiles of fragment emission from CH_3CN have been obtained. Both the C_2 $d^3\Pi_g$ Swan and the CN $B^2\Sigma^+$ Violet Systems have been observed. The populations develop with characteristic pressure dependent formation rates which are linear in pressure and linear in additive methane. Alternative kinetic hypothesis are:

i. Initial two-quantum excitation of a bound state of the parent, $3^1A''D$, and subsequent predissociation through competing unimolecular and collisional processes.

ii. Prompt scission yielding CN fragments in the ground electronic state $X^2\Sigma^+$ but with very high levels concomitant vibration (a 'dark channel') extending above the emissive B state. This would then be followed by collisional crossing to the B state - essentially an inverse conversion. There is some basis for such an hypothesis in observations and interpetations within the literature and in some observations of our own.

We are currently studying isotopic materials $^{12}CH_3{}^{13}C^{14}N$, $^{12}CH_3{}^{12}C^{15}N$, and $^{13}CH_3{}^{13}C^{14}N$, as well as normal $^{12}CH_3{}^{12}C^{14}N$. With these compounds we expect to obtain valuable information similar to that found with acetylene. For instance, we believe that the CN fragment derives only from the cyano group of the parent and that the C_2 fragment originates from carbons in the parent methyl groups. Preliminary work with HCN indicates that C_2 is not formed, though CN is abundent.

D. Photolysis of Gas-Phase Nitromethane

While the single beam experiments described previously have proven to be quite fruitful in elucidating processes involving excited-state products, they provide no information about the non emissive ground-state fragments. These fragments might well be the major products of the fast energetic reaction under study. As a consequence, a two-beam excite and probe experiment has been undertaken during the past year. The experiment utilizes a Nd:phosphate glass laser system in which the 4th harmonic at 264 nm dissociates the molecule under investigation and a second beam at 527 nm probes for the absorption of the fragments utilizing the technique of laser-induced fluorescence. The laser system was perfected during the past year and has been applied to study the gas-phase photolysis of nitromethane.

The fluorescence signature of the expected NO_2 fragment was first determined in NO_2 vapor before attempting the nitromethane photolysis experiments. The observed fluorescence decay curves could be constructed from single-exponential fits and were consistant with previously published work on NO_2. It was found that pressures of > 5 torr nitromethane strongly quenched NO_2 fluorescence. Therefore, the two beam photolysis experiment was conducted at pressures between 0.1 and 2 torr.

Nitromethane was then photolysized and probed for ground-state fragments with the 527 nm pulse. Induced fluorescence was observed which was identical in spectral and temporal behavior to that observed in NO_2/nitromethane mixture studies. The formation kinetics of the attributed NO_2 fragment were investigated by varying the delay time between the 264 nm and 527 nm pulses. A sharp step in the intensity of the induced fluorescence vs. delay was observed. The position of the onset and rapid rise in signal appear to indicate extremely rapid (< 20 ps) formation of the fragment. The fluorescent signal was found to be linear in UV excitation and probe laser energy indicating dissociation from the lowest energy $n \rightarrow \pi^*$ transition of nitromethane.

The papers that have resulted from the work described above are included in the following pages. In the coming year work will proceed on the development of the species identification techniques. One technique that looks particulary promising is the recent development in our laboratory of a picosecond-white light CARS [coherent-antistokes Raman scattering] technique in which for the first time an entire Raman spectra can be observed with one picosecond laser pulse. We are now investigating the applicability of this technique to the study of energetic reactions.

TIME-RESOLVED C_2 SWAN EMISSION FROM SHORT-PULSE UV FRAGMENTATION OF CO: EVIDENCE FOR TWO C_2 FORMATION MECHANISMS

W.L. FAUST, L.S. GOLDBERG
Naval Research Laboratory, Washington, DC 20375, USA

and

B.B. CRAIG and R.G. WEISS
Department of Chemistry, Georgetown University, Washington, DC 20057, USA

Received 6 May 1981, in final form 30 June 1981

We have studied C_2 Swan ($d\,^3\Pi_g \rightarrow a\,^3\Pi_u$) emission resulting from multiphoton UV excitation of CO. Population of $d\,^3\Pi_g$ proceeds through distinct early and late processes, the former giving rise only to normal Swan emission. The late process is responsible for $v' = 6$ enhancement (high-pressure bands), and it dominates time-averaged emission in all bands for >10 Torr of CO.

1. Introduction

The Swan band emission systems of C_2 ($d\,^3\Pi_g \rightarrow a\,^3\Pi_u$) are well known for their prominence in flames and appearance under diverse conditions of excitation [1]. C_2 Swan band emission from pulsed excitation of CO includes the high-pressure bands of Fowler [2], now attributed to an enhancement of $v' = 6$. The very identification of the spectroscopic anomalies as components of Swan emission [3] and the peculiar population kinetics [4,5] have afforded challenge to analysis. CO is not entirely unique in producing such features. Several other systems (with parents not necessarily containing oxygen atoms) necessitate distinct reaction schemes. The current understanding of the excess $v' = 6$ population has depended heavily upon high-resolution spectroscopy and term analysis [6,7], and upon potential-curve calculations [8,9]. Although investigated for many years, the origin of the normal and high-pressure Swan emission remains unresolved.

In the current work, we have studied the spectral and temporal development of band and line emission from photolysis products, subsequent to multiphoton 266 nm excitation of CO (5 – 100 Torr) with a 25 ps pulse. Through signal digitization and averaging, records have been obtained over a time scale ranging from a subnanosecond detection risetime to over 50 μs. It is found that excitation of Swan band emission occurs through two distinct mechanisms, *early* and *late*. The high-pressure bands arise only from the late process.

2. Experimental

Excitation was provided by the fourth harmonic of a mode-locked Nd:YAG laser system [10]. The 266 nm single pulse (≈ 10 mJ, 25 ps) was focused into a static gas cell with LiF windows, producing flux densities in excess of 10^{11} W cm^{-2}. Emission was collected at right angles and focused into a Jarrell–Ash 1 m spectrometer (resolution 1 nm). The instrument was coupled at the exit slit to a Varian VPM-154M crossed-field photomultiplier (GaAs, spectral range 200–900 nm, 0.15 ns risetime), or through a side mirror to an EG&G OMA II 500 channel intensified (ISIT) vidicon system. The intensifier section of the vidicon could be gated by a high-voltage pulse generator triggered from the laser pulse. Time-resolved waveforms from the photomultiplier were signal-

averaged (e.g. 64 shots) by a Tektronix 7912 AD digitizing oscilloscope (system step-function risetime 0.85 ns) interfaced to a Tektronix 4052 computer. Background and instrumental irregularities were subtracted by use of the computer system, e.g. emission bands generally are represented by the difference between signals at the band head and ≈ 1 nm to the red.

Carbon monoxide was ultra-high-purity grade (Matheson) and was freed of any metal carbonyl contaminants [11]. Pressures were measured by a Wallace Tiernan gauge (± 0.1 Torr). No evidence of changes in the temporal or spectral distribution of emission due to formation of stable photolytic products was observed during a typical series of several hundred pulses (firing rate $\frac{1}{2}$ Hz).

3. Results

3.1. Photolysis spectra — normal Swan and high-pressure features

The Swan bands of $C_2(d\,^3\Pi_g \rightarrow a\,^3\Pi_u)$ present violet-degraded heads (v', v'') spanning much of the visible. Spectral and kinetic observations by others support two classifications for C_2 emission: normal Swan bands associated with $v' = 0$–6, and high-pressure Swan bands associated with an excess population $v' = 6$ [1–7]. Vibrations $v' \geq 6$ correspond to headless or tail bands which are not evident in any of our current observations. Photolysis of many simple gases (e.g. C_2H_2, CH_3CN, CH_4) yields only the normal Swan bands [10,12]. Fig. 1a is a time-averaged C_2 $\Delta v = +1$ spectrum from 25 Torr of CH_3CN. No exceptional intensity is associated with $v' = 6$. This Swan emission is fully developed very early after excitation (within a few nanoseconds) and persists less than 200 ns [12]. All vibrational rotational features of these Swan bands share a common time development for a given gas and pressure.

Curves b and c in fig. 1 are time-gated vidicon spectra from 25 Torr of CO. For b, signal was accepted throughout an interval of 900 μs after the laser pulse (so that no emission was rejected) and is typical of reported time-averaged C_2 spectra produced from a CO discharge [6,7]. Swan emission following CO photolysis displays less rotational excitation than is typical of other parent molecules. This effect can be

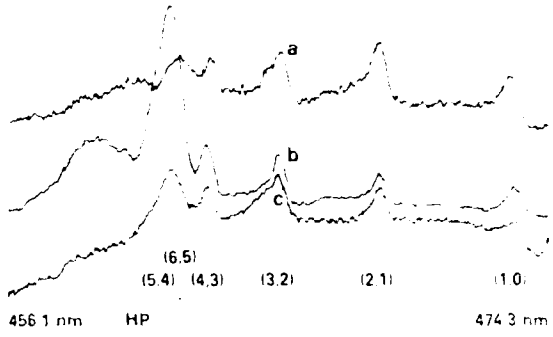

Fig. 1. Signal-averaged vidicon spectra of C_2 Swan emission ($\Delta v = +1$). (a) 25 Torr of CH_3CN, no gating, 50 laser pulses. (b) 25 Torr of CO, 900 μs gate, 20 laser pulses. (c) 25 Torr of CO, 1 μs gate, 500 laser pulses. Note that the high-pressure system is double-headed; both bands are absent in spectrum (c).

recognized in comparison of figs. 1a and 1b, but it is more evident with better resolution and with baseline subtraction [7,10]. In fig. 1b, the (6,5) high-pressure band is very prominent, 0.18 nm to the red of the (5,4) band head[3].

For curve c of fig. 1 the intensifier gate was set to accept signal for an interval of 1 μs following the laser pulse. To obtain adequate signal-to-noise within this limited gate interval we accumulated signal from 500 laser pulses. The normal Swan emission is present at this early time, but the high-pressure band is essentially absent. Clearly, there are at least two distinct mechanisms for excitation: an early one developed within ≤ 1 μs and another which assumes importance at later times.

3.2. Time development of spectral features

For illustration of the gross temporal features, figs 2a and 2b display digital oscilloscope traces recorded at low sweep speed, over a CO pressure range of 15–60 Torr. Here, the normal Swan systems are represented by the intense (0,0) band head at 516.3 nm, which is well isolated. As an example of the high-pressure system we have selected the (6,8) band head at 589.9 nm, which is better isolated than the (6,5) head shown in fig. 1 but is still underlain by a minor

[3] The band head assignments are taken from the high resolution work of Meinel and Messerle [7].

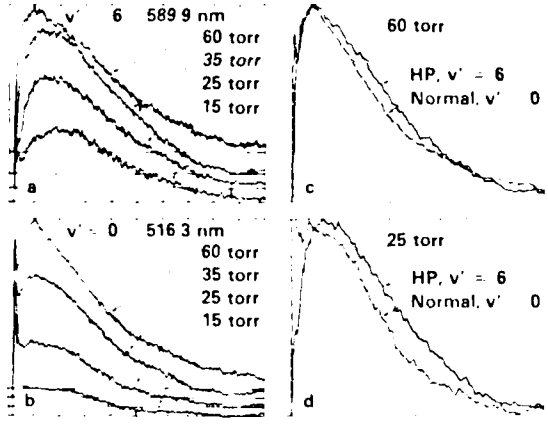

Fig. 2. Digital oscilloscope traces (signal average of 64 pulses) Comparison of normal and high-pressure C_2 emission profiles at a slow sweep speed (5 μs/div). (a), (b) Demonstration of gross indifference to CO pressure. (c), (d) Overlays to emphasize differences of $v' = 6$ and $v' = 0$ emission. For suppression of high-frequency shot noise, the data have been smoothed over 0.7 μs windows.

component of rotation attached to normal Swan heads (5,7), etc. The inference from the vidicon spectra of early and late processes is confirmed. For pressures ≥ 10 Torr of CO, the late process dominates time-averaged emission *i. both the normal Swan and* high-pressure bands. Apart from subtle differences of substructure, the duration of the late process is very similar for $v' = 6$ and $v' = 0$.

3.2.1. Early process

Figs. 3a and 3b resolve the time development of early Swan emission, (0,0) band head, for 25 Torr of CO. Since the C_2 d $^3\Pi_g$ collision-free lifetime is ≈ 120 ns [13], the comparatively slow decay process in fig. 3a reflects not the kinetics of the d $^3\Pi_g \rightarrow$ a $^3\Pi_u$ transition, but rather the destruction of a longer-lived precursor whose lifetime can be expressed simply as $\tau_1 = 1/k_1$ (where k_1 is a pseudo-first-order rate constant representing a sum of the rate constants responsible for loss of the precursor). The rise of the trace in fig. 3b is governed then by the loss of C_2 d $^3\Pi_g$. When the mean pulse energy is changed from ≈4 to 12 mJ, the risetime decreases. Hence, at least two processes must be considered to describe the loss of C_2 d $^3\Pi_g$: a bimolecular process (rate constant k_3) to account for

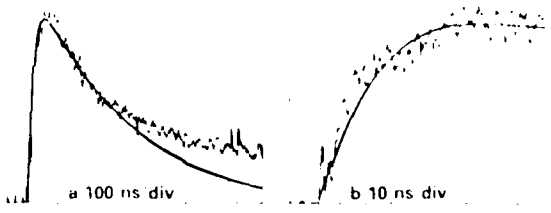

Fig. 3. Model curves fitting early process emission ($v' = 0$ at 516.3 nm), 25 Torr of CO. Two limiting τ_2 values (see text) have been employed.

the energy dependence and a pseudo-first-order decay (time constant $\tau_2 = 1/k_2$). k_2 is taken to be linear in CO pressure and to have a zero-pressure limit corresponding to $\tau_2 = 120$ ns. The proposed scheme is outlined by

$$X \xrightarrow{k_1} C_2 \text{ d } ^3\Pi_g \,, \tag{1}$$

$$C_2 \text{ d } ^3\Pi_g \xrightarrow{k_2} C_2 \text{ a } ^3\Pi_u \,, \tag{2}$$

$$C_2 \text{ d } ^3\Pi_g + T \xrightarrow{k_3} ? \,. \tag{3}$$

X represents an unspecified precursor. k_1 and k_2 each represent sums of first-order or pseudo-first-order rate constants describing the overall decay of X and of C_2 d $^3\Pi_g$ respectively. k_3 is the bimolecular rate constant for reactions of C_2 d $^3\Pi_g$ with itself or another transient of similar abundance. The above model allows satisfactory fits to the experimental curves over the range 5–60 Torr, where analysis is feasible. Two analyses were performed for each pressure, representing limits of no quenching ($\tau_2 = 1.2 \times 10^{-7}$ s [13]) and of strong quenching by CO. As a lower limit for τ_2, we employed a value extrapolated from data for quenching of C_2 d $^3\Pi_g$ by CH_3CN[#], according to $\tau_2 = \{(1.2 \times 10^{-7})^{-1} + k_Q[\text{CO}]\}^{-1}$ and $k_Q = 7.1 \times 10^8$ Torr^{-1} s^{-1} [12]. These extrema for τ_2, in curve fits to the initial fall of the traces at any given pressure, force no more than 10^{-7} change in τ_1. A plot of k_1

[#] We assume that CH_2CN is a more efficient quencher of C_2 d $^3\Pi_g$ than CO, since CH_3CN contains an unsaturated group similar to CO in addition to three reactive C–H bonds. Thus the k_Q value of CH_3CN [12] was adopted as an upper limit.

versus CO pressure is near-quadratic (τ_1 = 425 and 60 ns, at 5 and 60 Torr, respectively). At low pressures, the rise and decay curves can be fit adequately without a bimolecular term. In fitting the rise of the transient signal, k_3 is essential at 25 Torr and dominant above 35 Torr. The excitation conditions generate a spatially inhomogeneous concentration of emitting species. A consequence is that no simple significance can be attached to the absolute value of k_3.

3.2.2. Late process

In figs. 2a and 2b, neither the protracted rise nor fall of the emission intensity can reflect the *much* faster $d\,^3\Pi_g \rightarrow a\,^3\Pi_u$ emission kinetics. Clearly there are intermediate chemical species and/or state(s) of excitation preceding $C_2\,d\,^3\Pi_g$ formation.

Attempts to determine the dependence of the rates on fragment concentrations (hence, pulse-energy dependence) are compromised by the non-specificity of the excitation mechanism together with fluctuations of the laser pulse energy. Nevertheless, with variation of the excitation energy over an adequate range, the energy dependence of emission rise and decay times can be evaluated qualitatively. Such studies show that higher laser energy favors the late process, and the risetime of the late process is independent of pulse energy from ≈ 4 to 12 mJ. A simple kinetic treatment in terms of exponential time constants is not adequate to describe either the rise or the decay of the late process. However, the rate of rise is roughly proportional to CO pressure. The duration of emission from $v' = 0$ and from $v' = 0$ are not greatly different (fig. 2), which may suggest a common intermediate. The decay profiles are complex, though the structure is subtle, and they are not identical for $v' = 0$ and $v' = 0$ (figs. 2c and 2d). The shape features essentially belonging to the decay profile are insensitive to pressure (it must be recognized that the pressure-dependent *rate of rise* affects to some extent the apparent initial slope of fall).

As mentioned above, the normal Swan $C_2\,d\,^3\Pi_g$ populations produced from C_2H_2 and other simple gases develop rapidly, and they are rotationally hot [6,7,10,14], whereas from CO the time-averaged C_2 spectra are rotationally cold [7,10]. This suggests that for CO in the present study the early process may generate rotationally hot normal Swan emission which is masked on a time-averaged basis by a much

Fig. 4. [illegible] $C_2\,d\,^3\Pi_g$ [illegible] excitation [illegible] CO [illegible] $b_3\,^3\Pi_g - a\,^3\Pi_u$ [illegible] Here [illegible] last 828 ns [illegible]

larger rotationally cold population from the late process. In fig. 4, curve a measures the intensity of the (0,0) band head, where the rotational quantum numbers are relatively small. Curve b measures the intensity of associated rotation. There is an excess rotational intensity for the early component of the normal Swan emission (curve b), consistent with the above arguments, but the magnitude of this effect is not dramatic.

3.2.3. Other transients, species excluded from X

We have identified prompt emission from several other species: the atomic carbon line $3\,^1P^o \rightarrow 2\,^1S$ (247.8 nm), the C^+ line $3\,^2P^o \rightarrow 2\,^2S$ (283.7 nm), and the atomic oxygen lines $3\,^5P \rightarrow 3\,^5S$ (777.3 nm) and $3\,^3P \rightarrow 3\,^3S$ (844.6 nm). At 25 Torr of CO the C^+ line decays within 4 ns of the excitation pulse; it cannot be directly associated with the rise of C_2 emission at 247.8 nm, which peaks after ≈ 9 ns. The C line shows a non-exponential decay over ≳ 50 ns, whereas the radiative lifetime is only 2.8 ns [15]. At this pressure, we estimate the formation constant of $C_2\,d\,^3\Pi_g$, τ_1, to be ≈ 270 ns. Consequently, it is impossible for $C\,3\,^1P^o$ to be directly responsible for C_2 production. Similarly, neither $O\,3\,^3P$ nor $3\,^5P$ can play a direct role in C_2 formation, the decay constants are ≈ 15 ns at 25 Torr. However, the very appearance of these ionic and excited atomic systems clearly emphasizes the extreme nature of the excitation conditions. Production of $O\,3\,^3P$ from $CO\,X\,^1\Sigma^+$ requires at least 5 photons at 266 nm (≈ 20 eV). Several [illegible] components of CO or CO^+ emission were [illegible]

4. Discussion

The currently favored mechanism for the high pressure emission associates the abnormally high population of C_2 $d\,^3\Pi_g(v' = 6)$ with a perturbation of the $d\,^3\Pi_g$ state through a crossing by other electronic states [8,9]. The $b\,^3\Sigma_g^-(v = 19)$ state crosses $d\,^3\Pi_g(v' = 6)$ at rotational levels $v' = 19$ and 21 [6]. However, the work of Mentall and Messerle [7], based upon rotational analyses of high-resolution spectra, suggests that the $^1\Delta_g$ state could be responsible. Although the details of states and crossings are not firmly established, the mechanistic view is that initially produced higher states of C_2 (C_2^*) lead to abnormally high population of $v' = 6$.

Kunz et al. [16] have proposed a pathway for high pressure emission which involves C_2O as an intermediate

$$C + CO + M \rightarrow C_2O + M , \tag{4}$$

$$C_2O + C \rightarrow C_2^* + CO . \tag{5}$$

Wills and Devillers [17] have inferred a decay time of 20 μs for the disappearance of a red absorption, which they attributed to C_2O, in 400 Torr of CO. Very similar decay durations (≈ 20 μs) at all parent *for each pressure in the emission profiles of fig. 2*, and a further experiment at 100 Torr yielded essentially the same result evidently decay of the intermediate is not dependent upon collisions with the parent. Indeed, the late-term temporal profile may actually reflect the production and loss of the same intermediate as that observed by Wills and Devillers.

At the pressures employed here, depopulation of v' levels of $d\,^3\Pi_g$ should be dominated by quenching from the electronic state (e.g. $\tau_d \approx 20$ ns at 60 Torr). If initially $v' = 6$ were populated exclusively and relaxation to $v' < 6$ were to compete with the quenching process, then the decay profile of $v' = 6$ and $v' < 6$ emission would exhibit in detail the same shape. Figs. 2c and 2d indicate that there are reproducible differences between the shapes of the emission curves from $v' = 6$ and $v' < 6$. Consequently we favor parallel production of $v' = 6$ and $v' < 6$ levels.

5. Conclusion

[illegible] UV [illegible] CO [illegible] distinct populations of C_2 $d\,^3\Pi_g$ are generated. For [illegible] Torr of CO a late-term [illegible] is responsible for $v' < 6$ [illegible] also dominates the [illegible] that [illegible] vibrational [illegible] Swan [illegible] The high pressure [illegible] Swan [illegible] a [illegible] temporal [illegible] the [illegible] parallel [illegible] [illegible] $v' = 6$ and $v' < 6$, [illegible] from $v' = 6$. [illegible] C_2 [illegible] has been identified. The C_2 [illegible] is rotationally hotter than that of the high pressure state, characteristic of [illegible] Swan emission.

References

[1] R.W.B. Pearse and A.G. Gaydon, The identification of molecular spectra (Chapman and Hall, London, 1963).
[2] A. Fowler, Monthly Notices Roy. Astron. Soc. 70 (1910) 762.
[3] G. Herzberg, Phys. Rev. 49 (1942) 762.
[4] D.L. Baulch, A.E. Lewis, V.S. Reed and I.M. Campbell, J. Chem. Soc. Faraday Trans. 2 (1976) 520.
D.W. Naegelin and R.B. Palmer, J. Chem. Phys. 48 (1968) 2372, and references therein.
[5] L. Gosse, N. Sadeghi and J.C. Pebay-Peyroula, Chem. Phys. Letters 13 (1972) 587.
[6] J.B. Callen-more and A.C. Gaydon, Can. J. Phys. 42 (1964) 995.
[7] H. Mentall and C. Messerle, Astrophys. J. 184 (1973) 381.
[8] S.M. Read and F.E. Vanderslice, J. Chem. Phys. 36 (1962) 2366.
[9] K. Kuby and B. Lin, J. Chem. Phys. 73 (1980) 5893.
[10] R.B. Craig, W.E. Faust, L.S. Gilbert, P.E. Nelson and R.G. Weiss, in: Physics and plasma chemistry, Vol. 2, eds. R.M. Hochstrasser, W. Kaiser and C.V. Shank (Springer, Berlin, 1980) p. 253.
[11] W. Benker and A.E. Messerle, Mathematical Models (1972).
[12] R.B. Craig, W.E. Faust, L.S. Gilbert and R.G. Weiss, to be published.
[13] J.R. McDonald, L.A.P. Baronavski, A.M. [illegible] Chem. Phys. 53 (1978) 161.
[14] R. Brocklehurst and W.C. Swayze, J. Chem. Phys. 45 (1966) 3680.
[15] D.L. Mickey, Nucl. Instr. Methods 90 (1970) 77.
[16] C. Kunz, P. Battrick and S. Dodson, J. Chem. Phys. 46 (1967) 4157.
[17] C. Wills and C. Devillers, Chem. Phys. Letters 2 (1968) 51.

[illegible]

The primary dissociation channels in vacuum-ultraviolet photolysis of [illegible] have been inferred by analysis of the final products. [illegible] unidentified metastable state, denoted as $^3\Pi_0^{**}$, have been observed as important intermediates[1,2,3,4]. In the present investigation, we have [illegible] and developed a selective technique for [illegible] $^3\Pi_0$, formed exclusively in a [illegible] of the [illegible] of the present investigation is concerned with [illegible] possible excited species which is responsible for [illegible] Employing isotopic [illegible] and [illegible] photolysis, we have ascertained both unimolecular and bimolecular [illegible] $^3\Pi_0$. Parallel processes for $^1\Pi_1$ and $^1\Sigma^+$ are also considered. Dissociation energy for excited $^3\Pi_0$, consistent with $^3\Pi_1$ and $^3\Pi_2^{**}$ as intermediates, are discussed.

II. EXPERIMENTAL

Much of the apparatus has been described previously [5,6]. Ultraviolet pulses (266 nm, 25 ps) of up to 10 mJ energy were obtained by twice-doubling the amplified single-pulse output from an active-passive mode-locked Nd:YAG laser system. The photolyzing pulse was focused into a static gas sample cell by a quartz lens. A study of the focal region with a beam-scan device gave a representative beam diameter of 0.15 mm. Emitted light was collected through a side window and dispersed in a one-meter Czerny-Turner spectrometer. A Varian VPM-154M crossed-field photomultiplier (sapphire window, bialkali photocathode) provided a spectral range 200 - 900 nm, and a risetime 0.15 ns. Spectra were acquired and averaged, typically for 64 laser pulses, with a Tektronix 7912AD digitizing oscilloscope. The net risetime of the detection system was 1.5 ns. Data were processed with a Tektronix 4052 computer system. An OMA II EG&G vidicon also was available for acquisition of time-averaged spectra.

For measurements of emission lifetimes under higher time resolution, we employed an Electrophotonics Model 512 streak camera equipped with an S-20 Photochron II streak tube. The krytron trigger circuitry was modified to reduce sweep jitter. Traces were recorded by a Nuclear Data vidicon system interfaced to a Nicolet minicomputer. To obtain adequate signal levels, color glass filters were used to isolate certain molecular bands. For temporal reference, second-harmonic pulse pairs were provided via a second path to a distinct portion of the streak camera entrance slit. With the sample cell at atmospheric pressure, the first 532 nm pulse was brought into synchronism with the near-instantaneous rise of breakdown emission produced by the 266 nm pulse. The second 532 nm pulse was delivered with a delay set to 500 ps. The streak data were computer-averaged to improve the signal-to-noise of the weak emission. Because of trigger jitter, each streak trace and its corresponding reference were stored individually. The

traces were normalized to the response function of the streak camera and vidicon recording system. They were then shifted to a common timing mark and averaged.

Acetylene $H^{12}C^{12}CH$ was Matheson high-purity grade, further purified by repeated vacuum distillation from liquid nitrogen/n-propanol slush (ca. 148 K) to liquid nitrogen. $H^{13}C^{13}CH$ was used as supplied by Merck, Inc. The isotopic content of the heavy acetylene was ascertained to be 83.1% $H^{13}C^{13}CH$ and 16.9% $H^{12}C^{13}CH$; this is based upon an analysis by the supplier of isotopic acetaldehyde prepared from acetylene of the same batch.

III. RESULTS

Acetylene at pressures 1 – 10 torr was irradiated under the conditions described above. The triplet C_2 Swan system (430–670nm) was by far the strongest component of emission. Very weak singlet C_2 emission was observed in the Mulliken system $^1\Sigma_u^+ \rightarrow X^1\Sigma_g^+$ (230–240nm) and in the Deslandres-d'Azambuja system $c^1\Pi_u \rightarrow A^1\Pi_u$ (380–410nm) [7]. The CH systems $A^2\Delta \rightarrow X^2\Pi$ (430–490nm) and $^2\Sigma^+ \rightarrow X^2\Pi$ (314.5nm) were also quite evident. There was no emission from molecular species other than these two fragments. Molecular continua have been observed in other studies of acetylene photolysis [2,8,9], and continua have been found in our work with other parents [5,6]. Nevertheless, continuum emission was absent or minimal in the present work with acetylene. Monatomic emission was limited to a few lines; e.g. C (247.6 nm), H (656.3 nm), and C^+ (283.7 nm). The integrated intensity for each case was much less than for the diatomics.

A. Detailed Studies of C_2 Swan Band Emission

Figure 1 displays typical oscilloscope waveforms of the $\Delta v = +1$ Swan emission obtained from 5 torr of $^{12}C_2H_2$, illustrating similar shapes at two vibrational heads and amid rotation. The risetimes are instrumentally limited. These curves were obtained at relatively high excitation energy (ca. 12 eV). For decay beyond 80% of the maximum, they accept exponential fits with a time constant $\tau = 45$ ns. A plot of $1/\tau$ versus acetylene pressure accommodates a straight line through the zero pressure intercept ($\tau = 119$ ns [9]). The time histories in Fig. 1 therefore represent the residence time of individual C_2 $d^3\Pi_g$ molecules rather than the destruction of some longer-lived precursor (cf. in contrast ref. 10). The slope yields an estimate of the quenching constant of C_2 $d^3\Pi_g$ by C_2H_2, $k_Q = 0.92 \pm 0.1 \times 10^{-10}$ cm^3 s^{-1}.

Streak camera recording allowed a study of the rise of Swan emission with greatly extended time resolution. Since there was essentially no interfering

emission, denoted in 4(b) and corresponding to the filters (in Table) centered at the $\Delta v = +1$ and $\Delta v = 0$ Swan bands near 474 and 516nm. Fig.2 presents the temporal rise of C_2^* emission, from 1 torr of acetylene. The figure includes also the reference pulses and a fit of the rise of Swan emission by a model curve of the form $1 - \exp(-t/\tau)$, with $\tau = 215$ ns. Clearly, collisionless $^3\Pi_u$ formation, e.g. unimolecular dissociation, is implied.

To confirm this, we undertook a study of Swan emission from isotopically-labeled acetylene. On the basis of spectra from the literature [11], the $\Delta v = +1$ portion was selected for our detailed studies, the signal-to-noise and resolution of isotopic splitting being most favorable. Waveforms were acquired representing emission at increments of 0.2 nm over the range 471.1 to 475.1 nm, encompassing the (1,0) and (2,1) band heads for each of the three isotopic forms. The $^{13}C_2$ (3,2) band head is also present, but it is not effectively resolved from the $^{12}C_2$ (2,1) head. A total pressure of 5 torr was employed uniformly for the single-isotope materials and for a 1:1 $^{12}C_2H_2$:$^{13}C_2H_2$ mixture.

For the mixed-parent gas fills it was immediately apparent that the temporal emission profiles at the band heads of $^{12}C^{13}C$ were not identical in shape to those of the corresponding $^{12}C_2$ and $^{13}C_2$ heads. Qualitatively, the $^{12}C^{13}C$ heads exhibited an excess of emission during an intermediate interval of time, ca. 5 to 25ns after the laser pulse; the asymptotic decays, however, are alike. For a systematic display of this, spectra were constructed as follows: at each wavelength an integral of the emission waveform was taken over an "early" or a "late" interval of time (see Fig. 1; as measured from the laser pulse, early ~ ca. -2 to +3 ns and late ~ 13 to 42 ns). Such spectra were obtained for laser amplifier settings yielding two values of average uv pulse energy, ca. 7.5 and 12 mJ. In Fig. 3 two of the curves display low-energy early-interval spectra for the distinct parent gases. The third is a similar spectrum for the mixed parents.

At this low level of excitation, the early signal associated with the crossed isotope $^{12}C^{13}C$ is relatively small; i.e. the prompt product C_2 largely corresponds to the isotopic parents .

Figure 4 displays, for the equal mixture of parents, the four cases of energy and time interval. The progression of curves from low-energy/early to high-energy/late confirms the prompt (unimolecular) process asserted above and illustrates also a delayed (collisional) process in which the isotopes are scrambled.

In Figure 5 this point is developed in greater detail, by further manipulation of waveforms (data obtained at 5 torr, with ca. 12 mJ energy). The primary waveform at the wavelength of the $^{12}C^{13}C$ band head, 474.5 nm (curve a of Fig. 5), is not a direct history of the scrambling process: rotation attached to the $^{13}C_2$ band head at 475.3 nm underlies the $^{12}C^{13}C$ band head, and the heavy acetylene is not altogether pure. However, we have developed a procedure effectively to strip out the latter components of signal, employing waveforms at 474.5 nm and 475.3 nm from the heavy-isotope material to establish the relative signal at 474.5 nm due to these components. Curve c in the figure should then represent the collisional production of $^{12}C^{13}C$ due to the joint presence of both parent acetylene isotopes. Waveforms such as c were consistently reproducible. Such data also were gathered and analyzed for 8 torr and 2.5 torr of acetylene. The growing-in time was found to decrease with increasing pressure but was uniformly insensitive to the pulse energy; it is clearly indicated that this risetime is controlled by collisions of a precursor with the parent.

We have noted that the collisional process is [illegible] pulse energies (Fig. 4); it is possible to pursue this more quantitatively. For isotopically-pure parent gases at equal partial pressures, complete scrambling should yield $^{12}C_2$, $^{12}C^{13}C$, and $^{13}C_2$ in statistical ratio 1:2:1. At 12 mJ, even

the collisional C_2 formation is most prominent, all-time integrals were constructed of the excess $^1\Sigma_u^+$ signal (Fig. 5, curve c) and of the $^1\Pi_g$ signal. The ratio (potentially 2:1) was found to be 1.1:1, corresponding to 70% of total C_2 produced in the collisional process at this relatively high pulse-energy level.

The participation of two processes generating C_2 $^1\Pi_g$, prompt (unimolecular) and delayed (intermolecular), is regarded as established. It was long been recognized that under many conditions Swan emission exhibits high levels of rotational excitation [6,9,10,12]. Thus it is interesting to consider the possibility of distinct degrees of rotational or of vibrational excitation for the prompt and delayed processes generating C_2^*. This question is addressed in Fig. 6, where the data benefit from enhancement of the signal-to-noise ratio inherent in integral spectra. There is no indication of distinct levels of vibrational excitation; but the data points below 473.9 nm, associated with rotational excitation, are uniformly higher for the late-term integrals. Quantitatively, the signal-and-rotation relative to that at the band head is 2% greater for the late time interval. This modest enhancement of rotational excitation for the intermolecular process proved to be quite reproducible. The vidicon is incapable of gating at a speed appropriate for investigation of this issue by temporal separation. However, a spectrum at 25 torr shows more rotation than one at 5 torr; this is consistent with relative enhancement of the collisional process at the higher pressure, and with a higher level of associated rotation for the late collisional process. In a related study of ethylene with 10.6 μ pulses of 250 ns duration [12], a pressure dependence was observed for vibrational as well as for rotational excitation of C_2^* fragments.

Emission associated with high levels of rotation may be observed well to the blue of each band-head series [6,9] (i.e. for $\Delta v = +1$). In Fig. 7 we compare spectra obtained at 473.4 nm, the (1,0) band head, and at 468.5 nm, and rotation

associated with the entire Δv = +1 series. The apparent protracted formation of rotationally hot C_2^* reflects a larger fractional contribution of the collisional process, corroborating the inference from Fig. 6 (cf. also Fig. 5, curve e).

B. C_2 Singlet Emission

C_2 possesses a complex structure of electronic states, including singlets and quintets as well as triplets [14]. Several systems of emission are known [7], among triplet states and among singlets. The systems $c^1\Sigma_g^+ \rightarrow A^1\Pi_u$ (0,0 at 385.2 nm) and $b^1\Sigma_g^+ \rightarrow X^1\Sigma_g^+$ (0,0 at 231.3 nm) were observed, but the integrated intensity for each was $< 10^{-2}$ of that in the Swan system. The $b^1\Sigma_g^+$ signal appears within a time less than the instrumental limit of 0.6 ns. There is a delay for the maximum of $D^1\Sigma_u^+$ signal, which suggests a collisional formation mechanism. Each signal decays to 30% of maximum within 25 ns.

It is particularly interesting that McDonald et al. [9], photolyzing C_2H_2 (30 mtorr) with an ArF laser at 193 nm, reported the Phillips system ($A^1\Pi_u \rightarrow X^1\Sigma_g^+$, with 3,0 at 771.5 nm and 2,0 at 875.1 nm) to be ca. 10^3 stronger than the Swan system. We did not detect the Phillips system; a careful test led only to an upper bound on the intensity of such emission. A thorough treatment involves several considerations: the $A^1\Pi_u$ emission rate (small), the spectral sensitivity of detection (relatively flat), and the detectivity-threshold (pertaining in our work to instantaneous rather than to time-averaged signal). The finding is that the initial $A^1\Pi_u$ population is no more than 5×10^{-4} of the $d^3\Pi_g$ population; i.e. the relative Phillips population is $< 5 \times 10^{-4}$ of that found in the ArF work.

C. CH Emission

In less extensive studies, the rise of emission in the $^2\Pi$ A band (0,0 at 431.3 nm) was found to contain two components. At 1 torr there is a prompt rise to 60 % of the peak signal; a further increase occurs within

approximately 10 ns. The secondary formation process shows a definite pressure dependence. Unimolecular and intermolecular processes are implied in OH $A^2\Sigma$ formation, although we do not have supportive information from labeled isotopes. The curves accept exponential decay with characteristic times of 20 ns at 5 torr and 70 ns at 1 torr, corresponding to $k_Q = 2.8 \pm 0.5 \times 10^{-10}$ cm^3 s^{-1}.

The integrated intensity of the OH C band (0,0 at 314.4 nm) is similar to that of the A band. However, only a prompt component of formation is observed. At 5 torr the emission decays to 30% of the peak within ca. 15 ns. In contrast with the observation of Jackson et al. [15], no emission was observed in the B band (0,0 at 388.9nm) ; the integrated intensity was not greater than 5% of that for the A band.

IV. DISCUSSION

A. Unimolecular Dissociation Processes

The primary observations here directly establish the existence of a unimolecular dissociation process of acetylene yielding C_2 $d^3\Pi_g$. Such channels also are implied for C_2 $a^1\Pi_g$ and for CH $A^2\Delta$ and $c^2\Sigma^+$. The character and identity of the intermediates remain unresolved and present some challenging questions: e.g., does the process leading to the emissive species (cf. the 215 nm diffuse) represent dissociation from a sufficiently energetic state of the parent manifold, or is there additional excitation (necessarily within the pulse duration) of an intermediate fragment? Also, we must consider the quantum order of the dissociative motion and the role of resonant and nonresonant excitations.

Excitation at 266 nm (4.66 ev, 107 kcal mol^{-1}) is lower energy than the recognized onset of single-quantum absorption in acetylene at 237.7 nm [120]. There is evidence of a triplet state as low as 2.6 to 4.7 ev [121], so that single-quantum excitation cannot be excluded absolutely; but such a transition is both Franck-Condon and spin-forbidden. The vuv absorption spectrum of acetylene [118,119] displays the following features in near-coincidence with our D_0 = 224 kcal $mole^{-1}$: a "predissociated state $3s\sigma$ (213.8 kcal $mole^{-1}$), and two valence states of (213.6 kcal mol^{-1}) and π^* (213.2 kcal mol^{-1}).

We now consider the competing channels for a Franck-Condon $\pi\sigma^*$ state at 214 kcal mol^{-1}. Applying high resolution in a search for rotational structure in the energy, Wilkinson found none [118]. This lowers prompt (≤ 1.6 ps) coupling to other states, whether bound (internal conversion to a vibrationally excited ground state or to some other isoenergetic state) or dissociative. The pertinent thermochemical thresholds for decomposition are [20]:
$C_2(^1\Sigma_g^+) + H_2$, 124 kcal mol^{-1} and $C_2 + 2H$, 144 kcal mol^{-1}. Potential curve calculations [20] and spectroscopic studies [118] have failed to identify a vibrational state of C_2,

[illegible] ionization. Final product analysis by secondary ion mass spectrometry [illegible] yields no clear indication of photochemically eliminated [illegible]. Rather, elimination proceeds with a quantum efficiency of 0.8, in competition with stabilizing collisions. The predissociation threshold of the parent, $^1\Pi_g^{**}$ $^1\Sigma_u^+$. The first step in either channel must be vibrational [illegible], to be competitive. The H atom elimination is not accompanied by ionization, the latter process being [illegible] by the vibrational energy as observed by Wilkinson [15]. Nevertheless, thermal conversion is possible for $^1\Pi_g$, and it is believed that the energetic ground state should be that [illegible]. Thus it seems very probable that $^1\Sigma$ formation occurs within ca. 2 ps, whether from an electronic state at 7eV or from a vibrationally-hot ground state.

1. Barrier Excitation of $^1\Pi_g^*$, $^1\Pi_g^{**}$

With absorption of a third quantum (301 kcal mol^{-1}) by the parent molecule, H atom elimination is expected to proceed at an enhanced rate; the fate of the resultant $^1\Sigma$ is discussed in the following section. A competing process, which is thermodynamically allowed, is formation of CH $A^2\Delta$ ($^1\Pi_g$ + CH $A^2\Delta$ + CH $X^2\Pi$, 300 kcal mol^{-1} [16]. Colonna [10] has demonstrated such a channel at 300 kcal mol^{-1}, and it is likely that this is the mechanism of our unimolecular CH $A^2\Delta$ elimination. Production of CH $C^2\Sigma^+$ is also allowed for 3A ($^1\Pi_g$ + CH $C^2\Sigma^+$ + CH $X^2\Pi$, 320 kcal mole^{-1}. Simultaneous elimination of two hydrogen atoms in a concerted three-center fission is rejected. Although 301 kcal mol^{-1} exceeds the ionization limit of 292 kcal mol^{-1} [16b], there is evidence that the other processes are dominant [17]. At the low level, the H atom elimination and ionization processes may proceed at higher rates. However, our data convey a general deficiency of ionic oxidation, which suggests that other processes intercede. For instance, visible H^+ oxidation, seen in boiler soot flame

discharges [28], was not observed, nor were those additional [illegible] which might have been assigned to ions. It appears that [illegible] dissociative channels do not permit recognition of [illegible] (see, however, the discussion of collisional processes in Section IV).

2. Further Excitation of C_2H

The primary two-quantum H elimination from C_2H_2 [illegible] threshold. There is an ambiguity in the distribution of the excess energy between H atom recoil and the internal energy of the C_2H [illegible] excitation. Regardless of the energy content within the [illegible], absorption of two additional quanta is required to produce $A^2\Pi_i$, v'=0 ($C_2H \rightarrow C_2 + {}^1\Pi_g$, v' = 6 + H, 236 kcal mol^{-1}). C_2 $^1\Pi_g$ requires three additional quanta ($C_2H \rightarrow C_2\ ^1\Pi_g$ + H, 221 kcal mole^{-1}). C_2H has been established as a gas-phase photolysis product of C_2H_2 through observation of ESR signals in a rare gas matrix at 4 K [29]. In a theoretical analysis, Fish et al. [30,31] [illegible] $\pi \rightarrow \pi^*$ excitation to a specific acetylene precursor state, $^1\Sigma_u^+$, leading to C_2H $3^2A'$ and $2^2A''$. The expected (0,0) excitation energy is 0.7 ev or somewhat less, very close to the valence states postulated by Wildroon who also suggested a π excitation). Absorption [30] and emission [31] of C_2H were treated in extensive ab initio calculations. Excitation of C_2H at 2[illegible] nm is supported through $\pi \rightarrow \pi^*$ transitions, although the assignment is not complete in detail. Additional resonant absorption leading to further fragmentation i.e. to C_2^* is then probable. In successive H eliminations, if dissociation occurs through singlet C_2H_2, then doublet C_2H has the appropriate spin to account for the triplet Swan emission; but triplet C_2H_2 would allow either doublet or quartet C_2H.

In other studies of acetylene photolysis [2,8,9] broad structureless continua, tentatively ascribed to C_2H^* or to $C_2H_2^{**}$, have been observed both in absorption and in emission. The bent geometry of the upper C_2H state identified

and ratios N_{O_2}, will not affect the electron temperature by more than 10%.

b. Additional processes

Additional $N_2(A^3\Sigma_u^+)$ reactions have been established. Similar processes would imply that $N_2(B^3\Pi_g)$ and $N_2(a'^1\Sigma_u^-)$ are the precursors of each emission band. However, the quenching rate of these species is not necessarily limited by the present uncertainties of the emission intensities. In fact, lower values of specific quenching rate k_q are obtained even for pressures at the tail density of the present data ($p_{N_2} \approx 1$ Torr) than for $N_2(A^3\Sigma_u^+)$, viz. 1.2×10^{-17} cm^3 s^{-1}; and for $N_2(a'^1\Sigma_u^-)$, viz. 30×10^{-17} cm^3 s^{-1}. These values are substantially larger than a typical diffusion-controlled rate constant of 10^{-13} cm^3 s^{-1} [37], and even relatively large even for reactive radical or excited state species [38-40]. Ignorant states or ionic species, affording long-range attractive forces, could account for the large cross sections implied by the observed quenching rates. Alternatively, suprathermal fragment velocities may be involved.

The intermediate time component/concept poorly fits to exponential behavior. Thus, on an exploratory basis, an hypothesized formation rate proportional to $[N_2(a'^1\Sigma_u^-)]^2$ was used to construct model N_2^* emission profiles. Parameter convergence was difficult to achieve; nevertheless, the model curves still do not fully adequately the observed rapid rise.

V. [illegible]

[illegible] rapid vibrational relaxation of the initially-excited C_2H_2 ($\tilde{A}^1A_u$) to a lower-lying vibrational level of the $\tilde{A}^1A_u$ state. The absence of C_2 $d^3\Pi_g$ and C_2 $A^1\Pi_u$ production. The rapid vibrational relaxation of the initially-excited C_2H_2 ($\tilde{A}^1A_u$) is clearly an essential feature of one or more of the C_2 production processes. It is unclear [illegible] of C_2H_2 or of C_2H_2 [illegible]. The collisional process could be a [illegible] of [illegible] excitation in the collision frequency. Vibrational [illegible] C_2H_2 ($\tilde{A}^1A_u$) [illegible] to successive excitation in the case of [illegible] to the initial S_1 state. In the collisional process [illegible] C_2^* and C_2^*, [illegible] experience pressure-dependent [illegible] [illegible] of bimolecular reactions of [illegible].

The preferred intramolecular route to C_2^* is [illegible] as the scheme outlined by Okabe et al. [30,31]; a successive excitation by the [illegible] electron system of C_2H_2 and of the intermediate C_2H. A double two-photon nonresonant $\pi \rightarrow \pi^*$ absorption by C_2H_2, the first [illegible]. This elimination is not direct. It may occur initially at the initial absorption energy 21eV (in processing other than to $C_2H_2^{**}$, which is taken to be stable) or it may proceed from a vibrationally excited ground state formed via rapid internal conversion. Subsequent excitation is taken to occur through successive resonant $\pi \rightarrow \pi^*$ absorptions in C_2H, yielding C_2^*. Although our technique detects only emissive fragments, the assignment by Okabe [13] of a quantum yield of 0.3 to the process $C_2H_2 \rightarrow C_2H + H$ suggests that such C_2^* production may initiate via a major dissociative route of C_2H_2. The 215 ps risetime observed for C_2 Swan emission may then reflect predissociation of C_2H^*, or alternatively it may reflect a relaxation process from a higher triplet of C_2.

ACKNOWLEDGEMENTS

We thank Dr. E.J. Friebele for valuable cooperative effort in achieving the necessary interface between the Nuclear Data vidicon system which serviced the streak camera and the Nicolet minicomputer system employed for processing the data. This work has been supported in part by the Office of Naval Research.

REFERENCES

1. H. Okabe, J. Chem. Phys. 75, 2772 (1981).

2. H. Okabe, J. Chem. Phys. 62, 2782 (1975).

3. A. H. Laufer, J. Chem. Phys. 73, 49 (1980).

4. L. J. Stief, V. J. DeCarlo, and R. J. Marcotte, J. Chem. Phys. 42, 3113 (1965).

5. B. B. Craig, W. L. Faust, L. S. Goldberg, J. H. Jensen, and R. B. Weiss, Picosecond Phenomena, Vol. 2, eds. R. M. Hochstrasser, W. Kaiser, and C. V. Shank, Proc. 2d Int'l Conf. on Picosecond Phenomena, Aspen Co., Mass., May, June 18-20, 1980, Springer-Verlag, Berlin 1980, p. 253; see also references therein.

6. B. B. Craig, W. L. Faust, L. S. Goldberg, J. H. Jensen, L. B. Jensen, and R. B. Weiss, Fast Reactions in Energetic Systems, eds. C. Capellos and R. F. Walker, Proc. NATO Adv. Study Inst. Dynamics, Bressanone, Italy, 1-15, 1980, D. Reidel Publ. Co., Dordrecht Netherlands 1981, p. 419.

7. R. W. B. Pearse and A. G. Gaydon, Identification of Molecular Spectra, Chapman and Hall, London 1965.

8. K. H. Becker, D. Marks, and M. Schurath, Z. Naturforsch. 22a, 1777 (1967).

9. J. R. McDonald, A. P. Baronavski, and V. M. Donnelly, Appl. Phys. 33, 171 (1978).

10. B. B. Craig, W. L. Faust, L. S. Goldberg, and R. B. Weiss, Appl. Phys. [illegible] 83, 265 (1981).

11. R. K. Dhumwad and N. A. Narasimham, Pan. J. Phys. 46, 1954 (1964).

12. W. Lochte-Holtgreven, Z. Fur Physik 64, 443 (1930).

13. J. H. Hall, Jr., M. L. Ferguson, and W. A. Williams, J. Chem. Phys. 67, 2247 (1978).

14. M. Kinoy and R. Lin, J. Chem. Phys. 70, 493 (1979).

15. W. M. Jackson, J. B. Halpern, and C. S. Lin, Appl. Phys. Lett. 33, 109 (1978).

16. A. F. Kistiakowsky, Phys. Rev. 37, 276 (1931).

17. G. G. Barton and H. S. Hunziker, J. Chem. Phys. 57, 3684 (1972).

18. P. G. Wilkinson, J. Mol. Spectr. 2, 387 (1958).

19. T. Yamagami and K. Watanabe, J. Chem. Phys. 50, 3436 (1969).

20. P. Desgoulin, Chem. Phys. 11, 329 (1975).

21. A. H. Laufer and A. M. Bass, J. Phys. Chem. 83, 310 (1978).

22. Note that fluorescence is not ordinarily observed from acetylene. There is such a report for acetylene in an inert gas matrix: L. E. Brus, J. Mol. Spectr. 75, 245 (1979).

23. K. Evans, R. Schops, S. A. Rice, and H. Heller, Chem. Soc. Faraday Trans. [illegible], 856 (1973).

24. W. L. Hase and Yn-Fei Weng, J. Chem. Phys. 61, 4690 (1974).

25. C. F. Cleaves and W. L. Hase, J. Chem. Phys. 66, 1503 (1977).

26. V. H. Kiesler, J. A. Miller, and H. E. McNabb, J. Chem. Phys. [illegible], 2[illegible] (1973).

27. J. Krelle, A. Schmidt, and W. Thiel, Chem. Phys. Letters 79, 547 (1981).

28. A. E. Douglas and J. B. Morton, Astrophys. J. 132, 1 (1960).

29. H. B. M. Braun, K. I. Dimitrev, and W. Weltner, Jr., J. Chem. Phys. [illegible], [illegible] (1974).

30. S. Shin, J. B. Peyerimhoff, and R. J. Buenker, J. Mol. Spectr. 64, 167 (1977).

31. S. Shih, S. D. Peyerimhoff, and R. J. Buenker, J. Mol. Spectr. 74, 124 (1979).

32. J. Tellinec and A. B. Bernstein, J. Chem. Phys. 71, 1359 (1979).

33. T. Bond, M. J. Bourner, and R. M. Noyes, J. Chem. Phys. 75, 4837 (1981).

34. H. Heinz, J. Jortner, and A. Szöke, J. Chem. Phys. 46, 2214 (1967).

35. Some support is afforded by measurements of excimer intensity versus laser pulse energy, executed in the current work; the lowest power-law exponent was 1.6.

36. A very salient but indirect, of bottleneck effects may be found in the observations of Yoon et al.[33], upon photolysis of benzene. After an initial transient, the primary IR pulse was ineffective toward further fragmentation. The parallel or following visible pulse was quite effective.

37. W. H. Miller, Dynamical Effects of Van Vleck, Pennsylvania, N.J., 1966; p. 140, p. [illegible].

38. J. S. Cohen, L. F. Doyle, M. S. Lin, and J. E. Ribble, Jr., Phys. Letters [illegible], 1[illegible] (1978).

39. N. W. Rosnali and P. Perner, Z. Naturforschung 26a, 1768 (1971).

40. A. P. Baronavski and J. R. McDonald, Chem. Phys. Letters 56, 369 (1978).

41. L. Pasternack and J. R. McDonald, Chem. Phys. 43, 173 (1979).

42. V. M. Donnelly and L. Pasternack, Chem. Phys. 39, 427 (1979).

43. M. N. R. Ashfold, M. A. Fullstone, G. Hancock, and G. W. Ketley, Chem. 55, 245 (1980).

44. C. K. Luk and R. Bersohn, J. Chem. Phys. 58, 2153 (1972).

45. W. M. Jackson, J. Chem. Phys. 61, 4177 (1974).

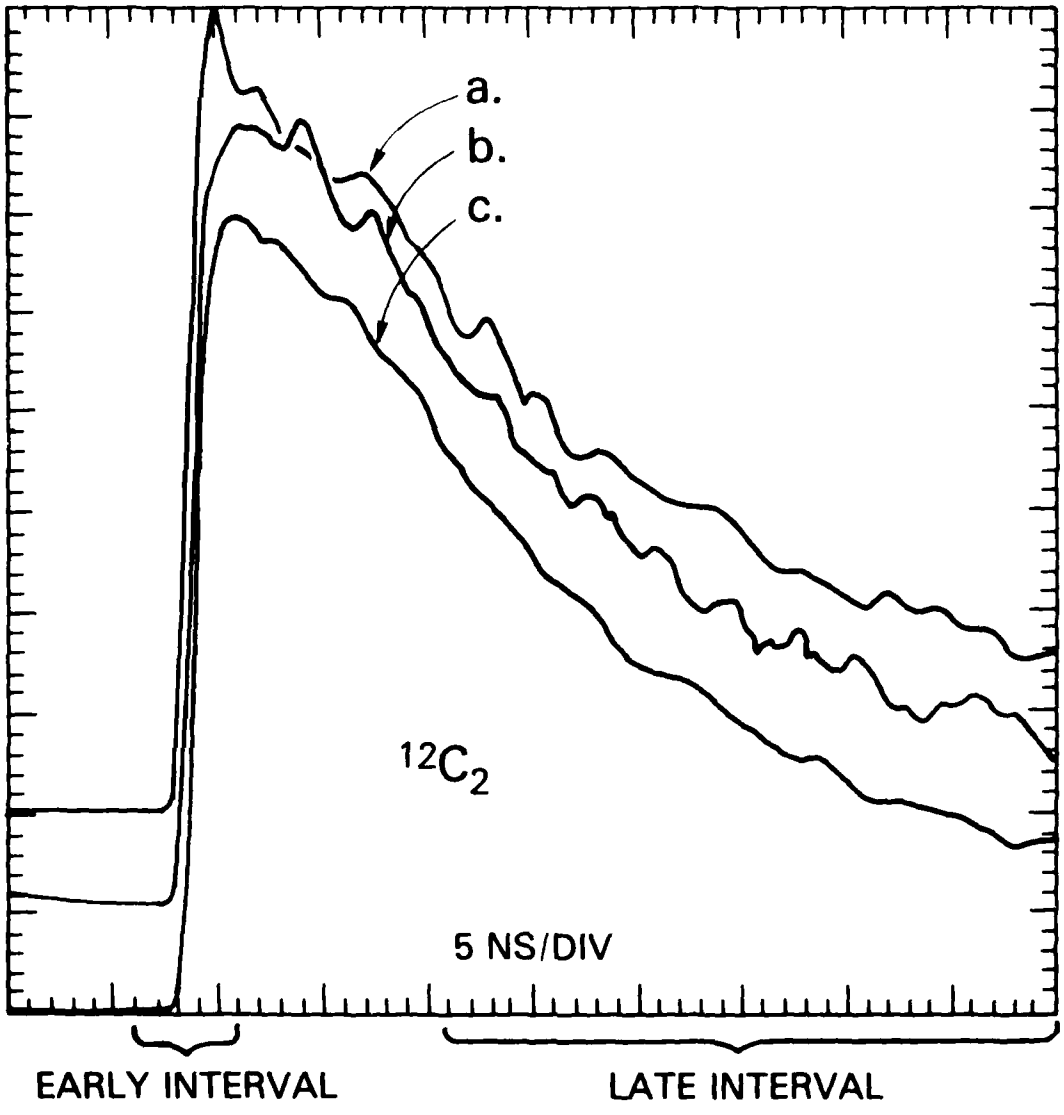

Figure 1

Comparison of temporal profiles for C_2 Swan emission at band heads and mid rotation; averages of 64 pulses.

The curves have been scaled to equal peak heights.

5 torr of $^{12}C_2H_2$; the same total pressure pertains for each figure.

uv pulse energy ca. 12 mJ.

a) (1,0) band head at 473.9 nm.
b) Rotation associated with the (1,0) head, at 472.7 nm.
c) (2,1) head at 471.7 nm.

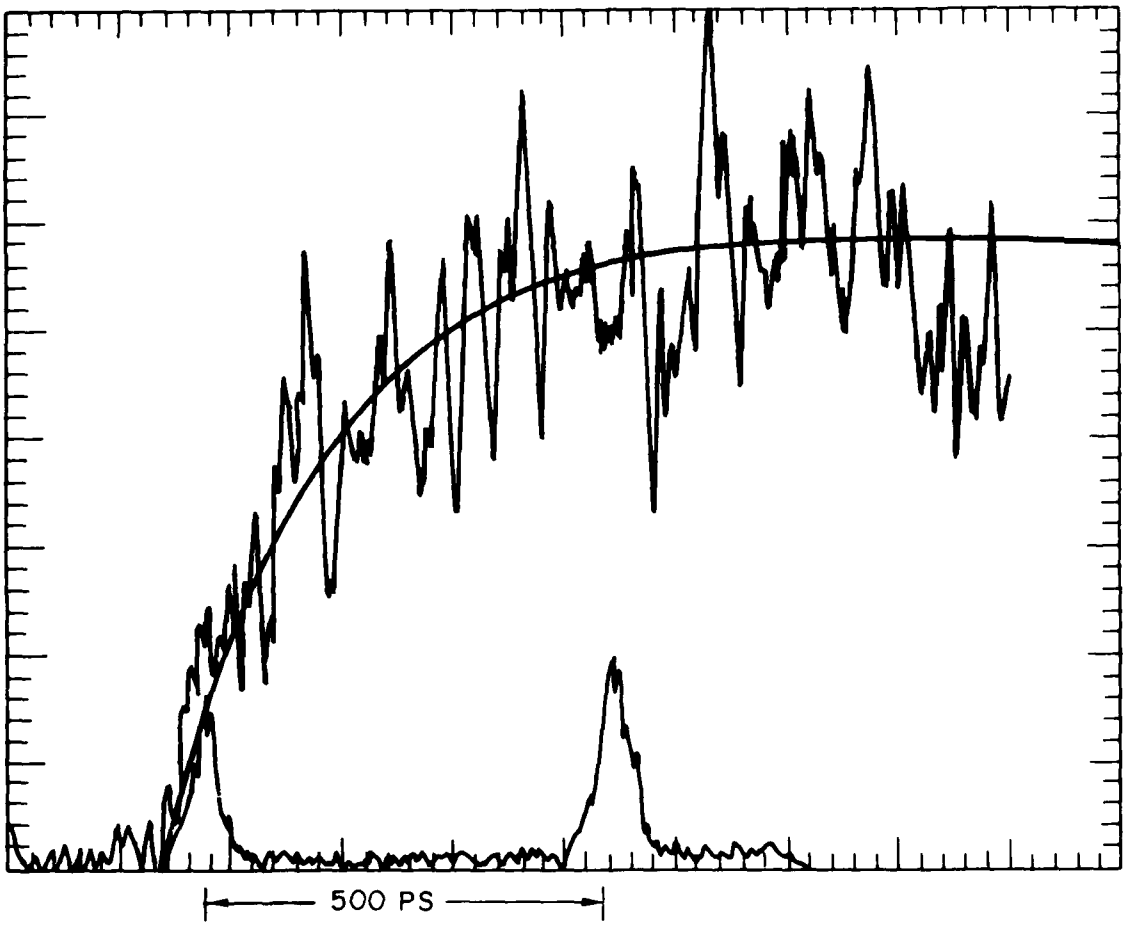

Figure 2

Streak camera record of the rise of Swan emission in the $\Delta v = +1$ and $\Delta v = 0$ bands; the average of 10 pulses.

Also shown are a model curve with time constant 215 ps, and second-harmonic reference pulses at a pair separation of 500 ps.

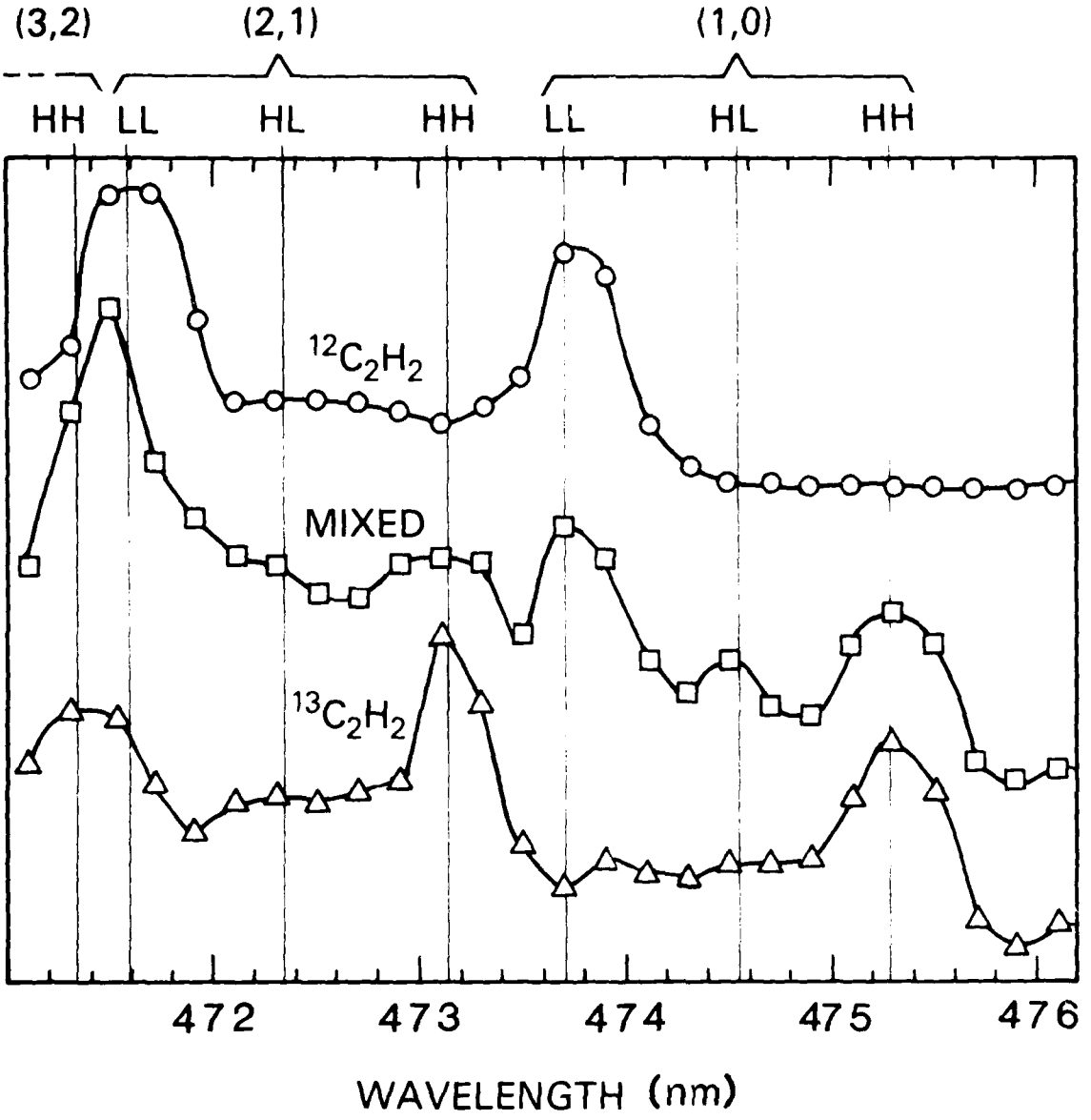

Figure 3

Spectra of early emission (first 5 ns; see Fig. 1) in the C_2 $\Delta v = +1$ Swan series; uv pulse energy ca. 2.5 mJ.

Curves for isotopically-distinct parent acetylenes, and for a 1:1 mixture of $^{12}C_2H_2$ and $^{13}C_2H_2$.

The notations HH, HL, and LL attached to band heads refer to heavy and to light isotopes of carbon.

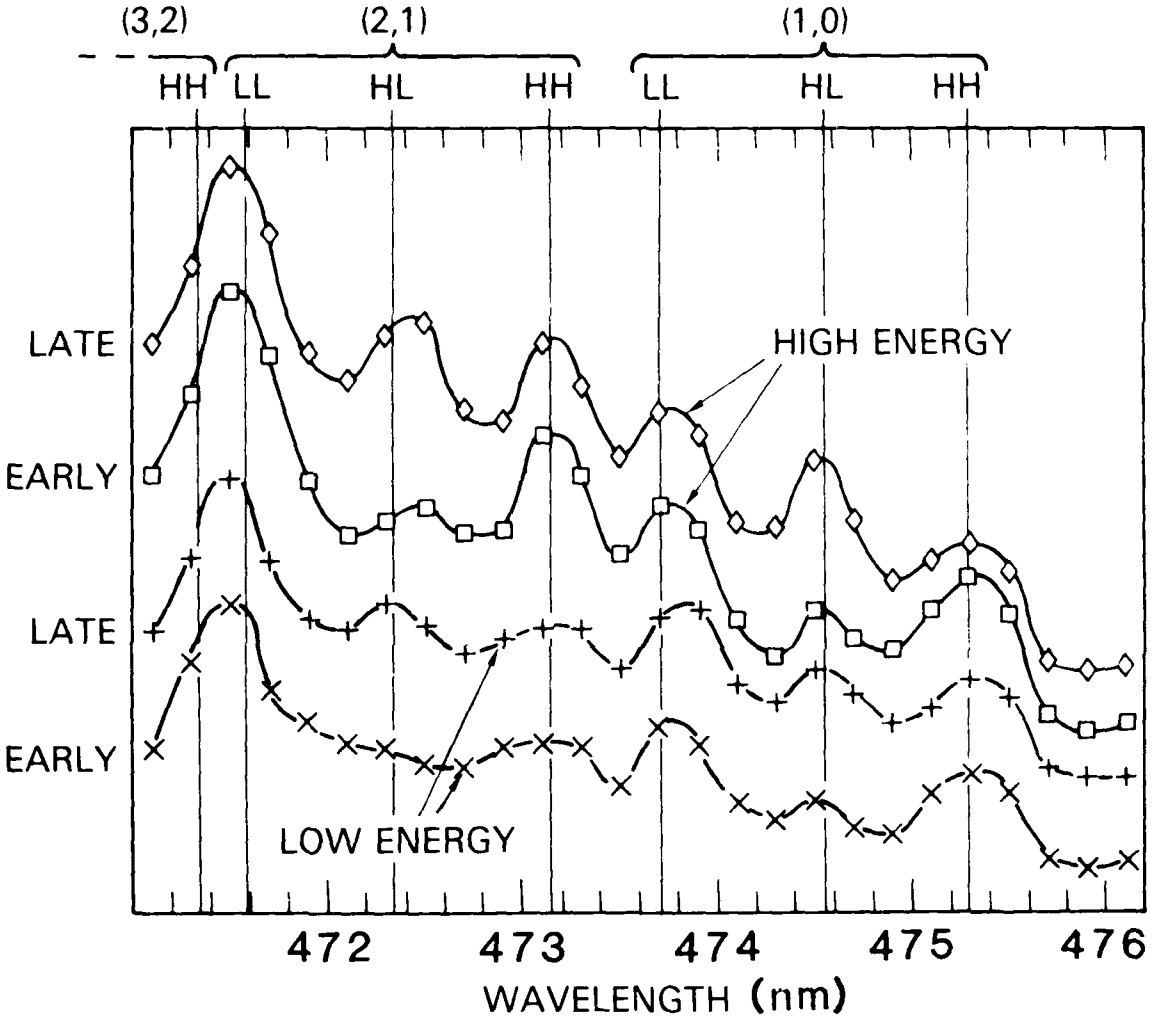

Figure 4

Spectra of Swan emission ($\Delta v = +1$) within early and within late intervals of time (see Fig. 1); curves for uv pulse energies ca. 2.5 mJ and ca. 12 mJ.

1:1 $^{12}C_2H_2$:$^{13}C_2H_2$ mixture.

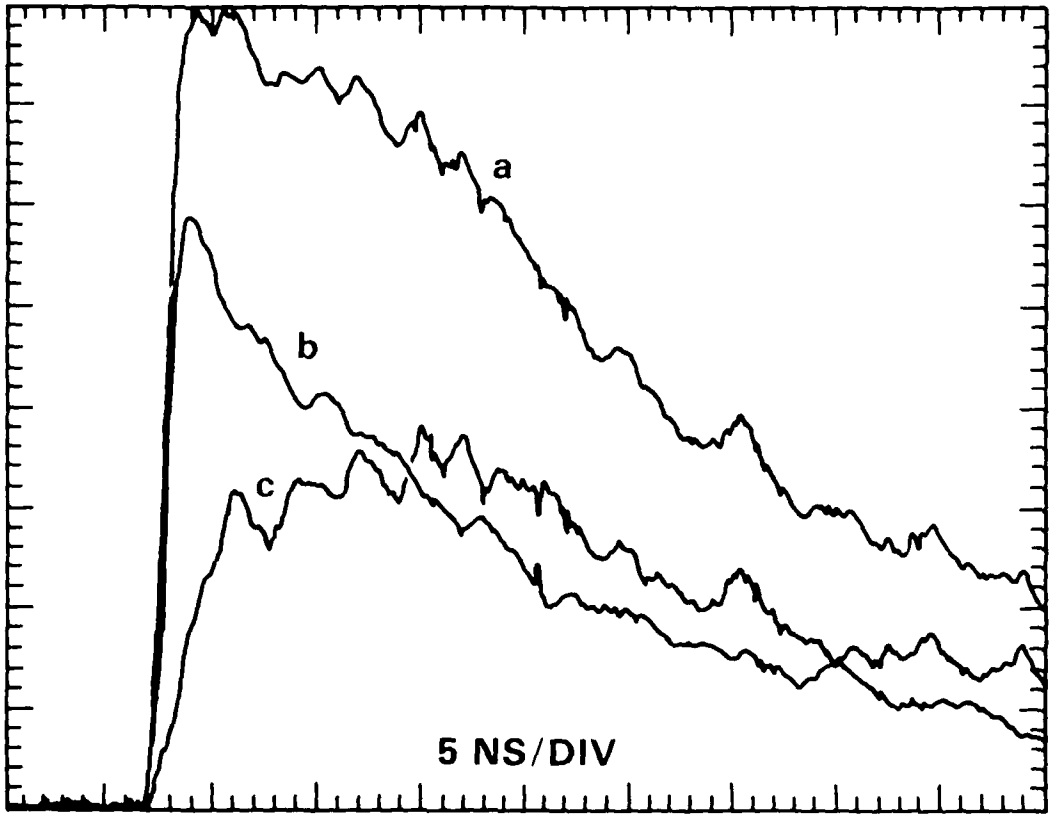

Figure 5

Construction of the time history of Swan $^{13}C\ ^{12}C$ arising in the collisional process; uv pulse energy ca. 12 mJ.

1:1 $^{13}C_2H_2$:$^{12}C_2H_2$ mixture.

a) Primary record of emission at the $^{13}C\ ^{12}C$ (1,0) head, 474.5 nm.
b) Reference waveform obtained by appropriate scaling of the emission record at the $^{13}C_2$ (1,0) head, 475.3 nm.
c) Subtraction of curve b from curve a, representing collisionally-formed $^{13}C\ ^{12}C$.

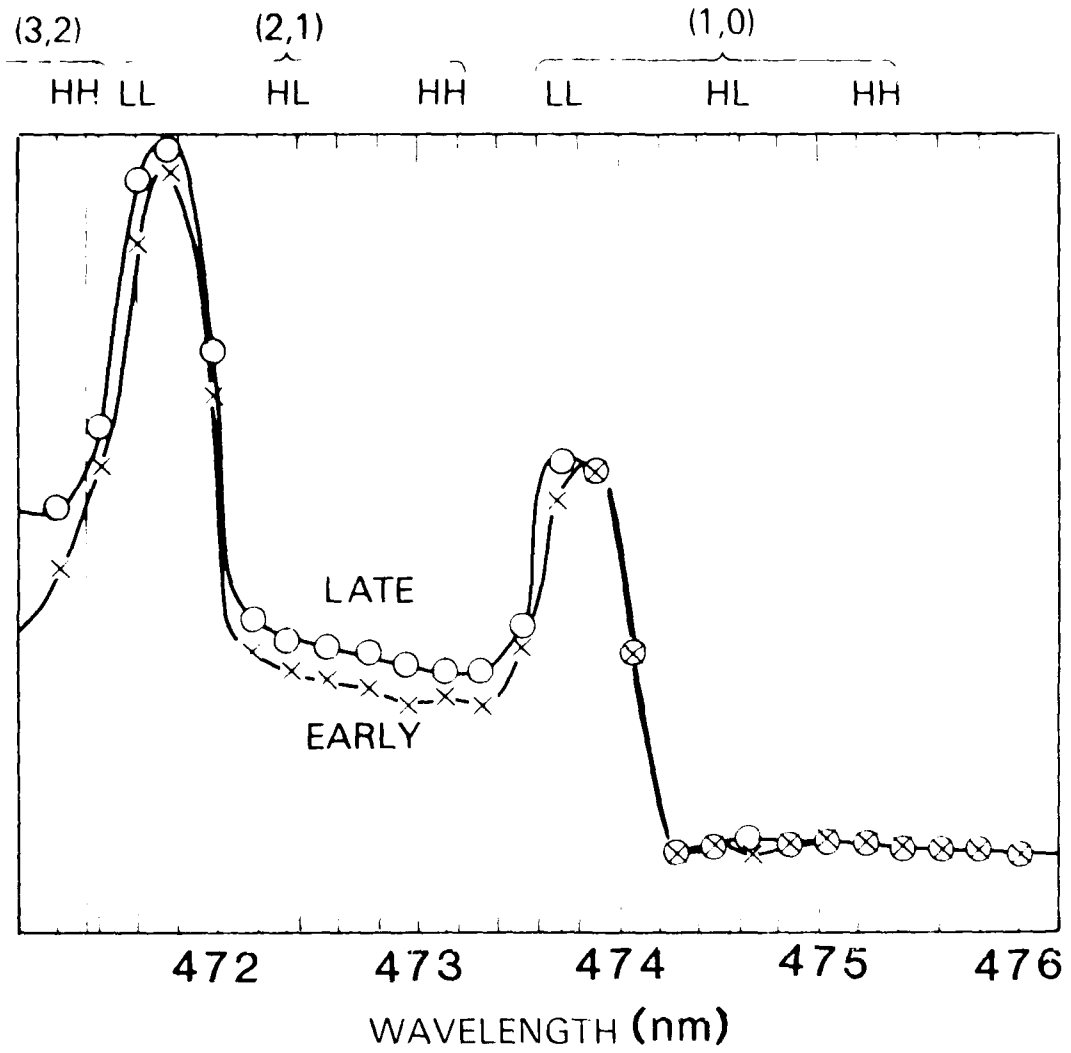

Figure 6

Comparison of vibrational/rotational distributions for early and late C_2 $d^3\Pi_g$ populations, $\Delta v = +1$ series; uv pulse energy ca. 12 mJ.

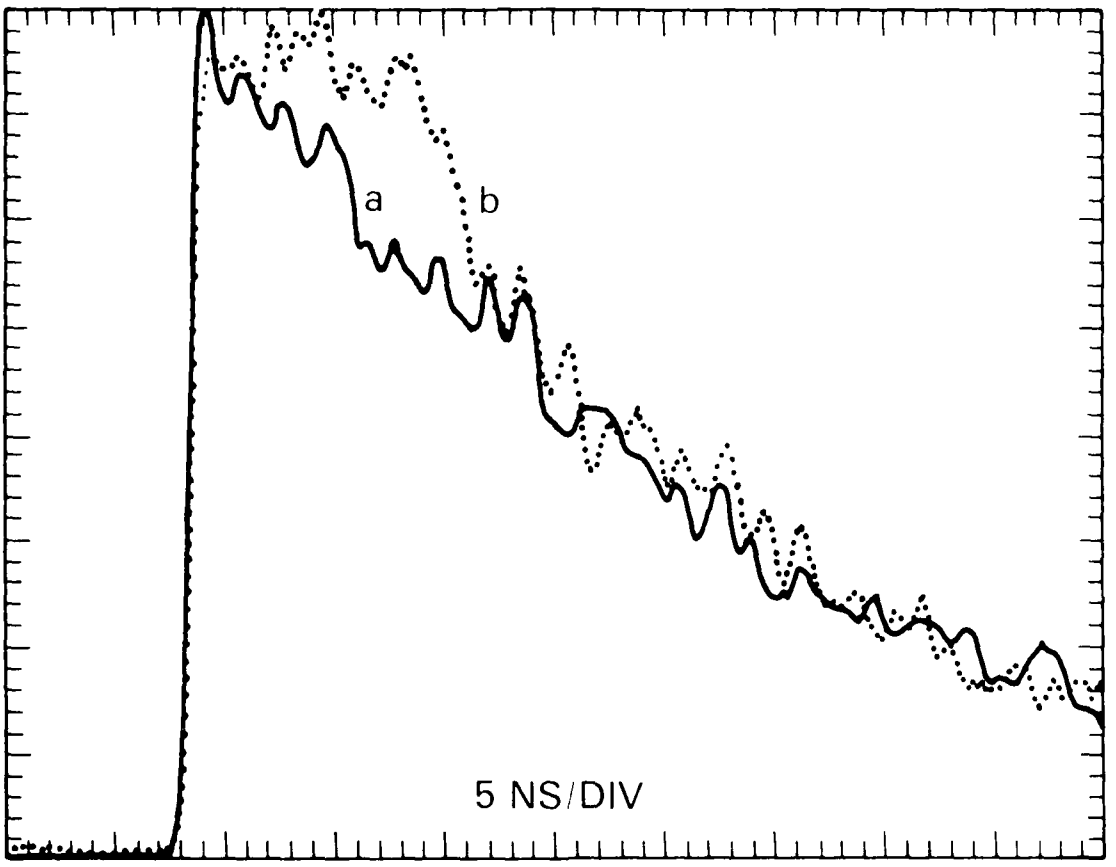

Figure 7

Comparison of temporal profiles for C_2 Swan emission amid states of high rotation and at a band head.

The curves have been scaled to a common late-term signal level.

a) 473.9 nm, the (1,0) band head.
b) 462.8 nm, hot rotation.

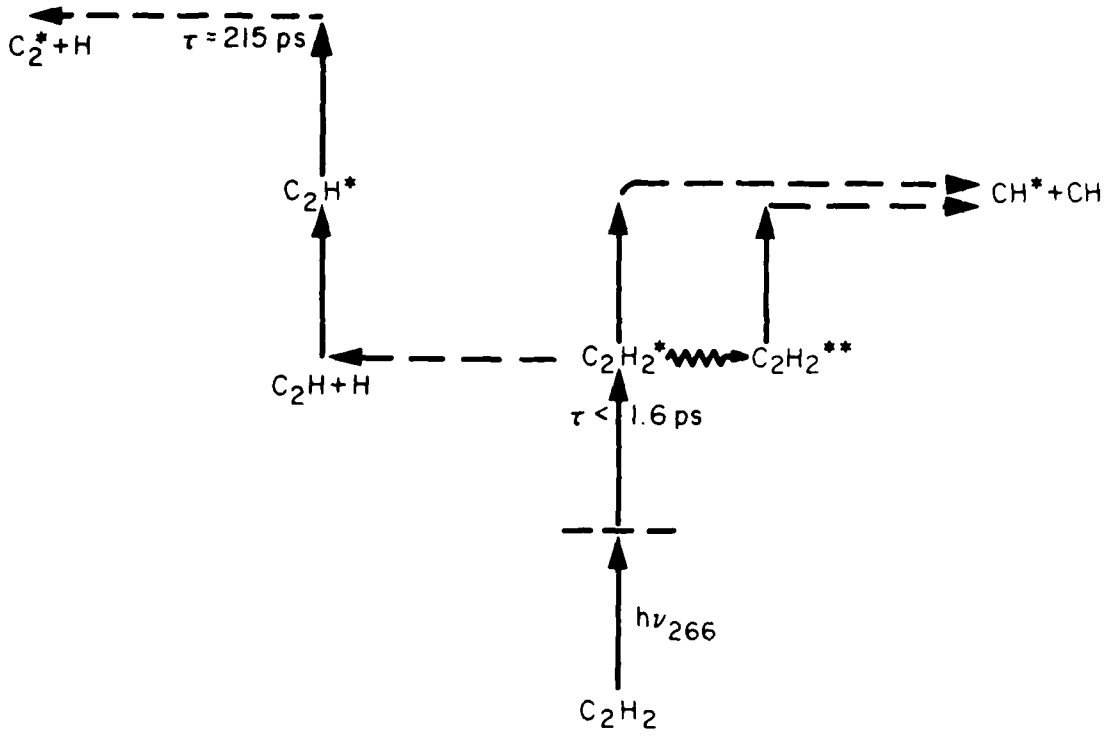

Figure 8

Schematic of preferred channels of $\pi \rightarrow \pi^*$ excitation (vertical arrows), intramolecular relaxation (wavy arrow), and unimolecular fragmentation (dashed arrows) for photolysis of C_2H_2 by 266 nm 25 ps pulses.

Picosecond UV Photolysis and Laser Induced Fluorescence Probing of Gas-Phase Nitromethane*

by

P. E. Schoen, M. J. Marrone, J. M. Schnur, and L. S. Goldberg

ABSTRACT

In a dual-beam picosecond experiment, we have performed UV photolysis of gas-phase nitromethane and have monitored the subsequent evolution of the NO_2 fragment population by laser induced fluorescence. The NO_2 radicals are formed promptly, within the ~ 5 ps pulse resolution of the experiment. Their population remains roughly constant for a probe delay time extending to 20 ns. The fluorescence intensity depends linearly upon both the photolyzing and the 527 nm probe pulse energies. The photolyzing 264 nm pulse itself generates some NO_2 in an excited fluorescing state.

* A preliminary account of this work was presented at the Xth International Conference on Photochemistry, The University of Iraklion, Crete, Greece, 6-12 September 1981; M. J. Marrone, P. E. Schoen, L. S. Goldberg, R. G. Weiss, J. M. Schnur and W. L. Faust.

The UV photolysis of nitromethane has been studied extensively for many years [1-9]. A number of authors have inferred, generally on the basis of chemical analysis of final products, that the primary photodissociation process leads to formation of the free radicals CH_3 and NO_2. However, identification of these fragments has been difficult because of their high reactivity. The first direct evidence for their presence among the photolysis products of nitromethane was provided by the electron paramagnetic resonance experiments of Bielski and Timmons [3]. Colles et al. utilized opto-acoustic detection to provide the first spectral identification of the NO_2 fragment from continuous photolysis of nitromethane [7]. More recently, laser techniques using UV [8,9] and multiphoton IR [10,11] excitation have led to the generation and detection of the NO_2 fragment. In the case of UV laser photolysis in the gas phase, Spears and Brugge observed vibrationally excited NO_2 fragments by means of laser induced fluorescence (LIF) on a microsecond time scale [8]. However, experiments by Kwok, et al., employing nano-second laser photolysis and mass spectroscopic fragment detection techniques observed no photodecomposition products [12].

In this letter, we report the first direct observation on a picosecond time scale of fragment formation in the UV photolysis of gas-phase nitromethane. Using a dual-beam experiment with LIF probing, we have determined that NO_2 fragments, identified from their fluorescence spectrum and quenching kinetics, are generated promptly by the UV excitation, within the 5 ps pulse resolution of the experiment.

This supports assignment of the observed reaction as:

$$CH_3NO_2 \xrightarrow{h\nu} CH_3 + NO_2 \qquad (I)$$

Experiment

Our nitromethane samples were obtained from Baker reagent grade material, which we distilled under nitrogen, collecting the middle fraction, b.p. 101 - 102°C. Individual samples were degassed by several freeze/thaw-vacuum pumping cycles. Samples of 0.1 to ~ 3.0 Torr pressure were loaded into a 15 cm diameter stainless steel cell whose interior walls had been coated with black Teflon to reduce scattered light. The entrance and exit cell windows were of lithium fluoride, and internal baffling was provided to prevent window fluorescence induced by the laser pulses from reaching the photodetector. Light emitted at 90° from the laser path was collected by a lens and focused through long-wavelength-pass color filters onto a slit in front of an EMI 9658 phototube. The tube had an S-20 photocathode (red sensitive to ~ 900 nm) and a pulse response (FWHM) of ~ 20 ns. The signal was processed by a Tektronix 7912AD digitizing oscilloscope coupled to a Tektronix 4052 computer for time integration of waveforms, and for data manipulation and storage.

The laser was a passively mode-locked Nd:phosphate glass oscillator/amplifier system [13] which generated 1054 nm single pulses typically of 5 ps duration and ca. 25 mJ energy at a repetition rate of 1/5 Hz. The IR pulse was frequency-doubled twice to give a photolyzing UV pulse energy of up to 3 mJ at 264 nm. The residual IR pulse energy was separated from the direct laser path by a beam splitter and was frequency-doubled independently, to give a probe pulse of up to 10 mJ at 527 nm. The probe pulse was directed along an optical delay line, and subsequently recombined co-axially with the photolyzing pulse. Both pulses were then sent into the sample cell without focusing, giving a photolyzing beam diameter of ~ 4 mm. Pulse energies were recorded on each shot, and were used to normalize the observed sample fluorescence data. The temporal and spectral quality of the pulses were monitored as the experiment

progressed by a two-photon fluorescence cell/vidicon and by a 0.5 meter spectrograph/Reticon array.

The zero time delay between the UV and probe pulses was determined by a photobleaching measurement in which the two pulses were focused into a thin cell filled with rhodomine 6 G dye solution. The UV pulse depopulated the dye ground state sufficiently that a weak probe pulse arriving after the UV pulse was transmitted.

Results

Figure 1 shows two representative traces of fluorescence intensity versus time, averaged over 8 laser shots, for a nitromethane pressure of 2.5 Torr. The lower trace shows the fluorescence signal for the UV photolyzing pulse alone. The upper trace was generated by a UV pulse plus a 527 nm probe pulse delayed by ~ 200 ps. A probe pulse alone produced virtually no signal either initially or after hundreds of UV shots into the cell. The emission in Fig. 1 was filtered by a Corning 2-73 filter, which transmits wavelengths longer than ~ 560 nm. While the UV pulse itself obviously produces a fluorescing fragment, input of the 527 nm pulse has increased the fluorescence intensity roughly 3-fold. The observed fluorescence has a risetime that is phototube-limited; its decay shows a single exponential fall time which is strongly dependent on gas pressure. The decay time for the UV-only case is roughly the same as that for UV + probe. The integrated fluorescence intensity reaches a maximum at about 10 Torr. of nitromethane, but the quenching rate at this pressure is too fast to be resolved with our phototube.

The collision free (1 m Torr) lifetime reported for NO_2 fluorescence is approximately 55 μsec [14]. At our lowest nitromethane pressure of ~ 100 mTorr observe a decay time of ~ 1.5 microseconds. The emission is more rapidly quenched at still higher pressure; at 2.5 Torr the decay time was ~ 70ns. A Stern-Volmer plot of decay rates versus pressure is linear over

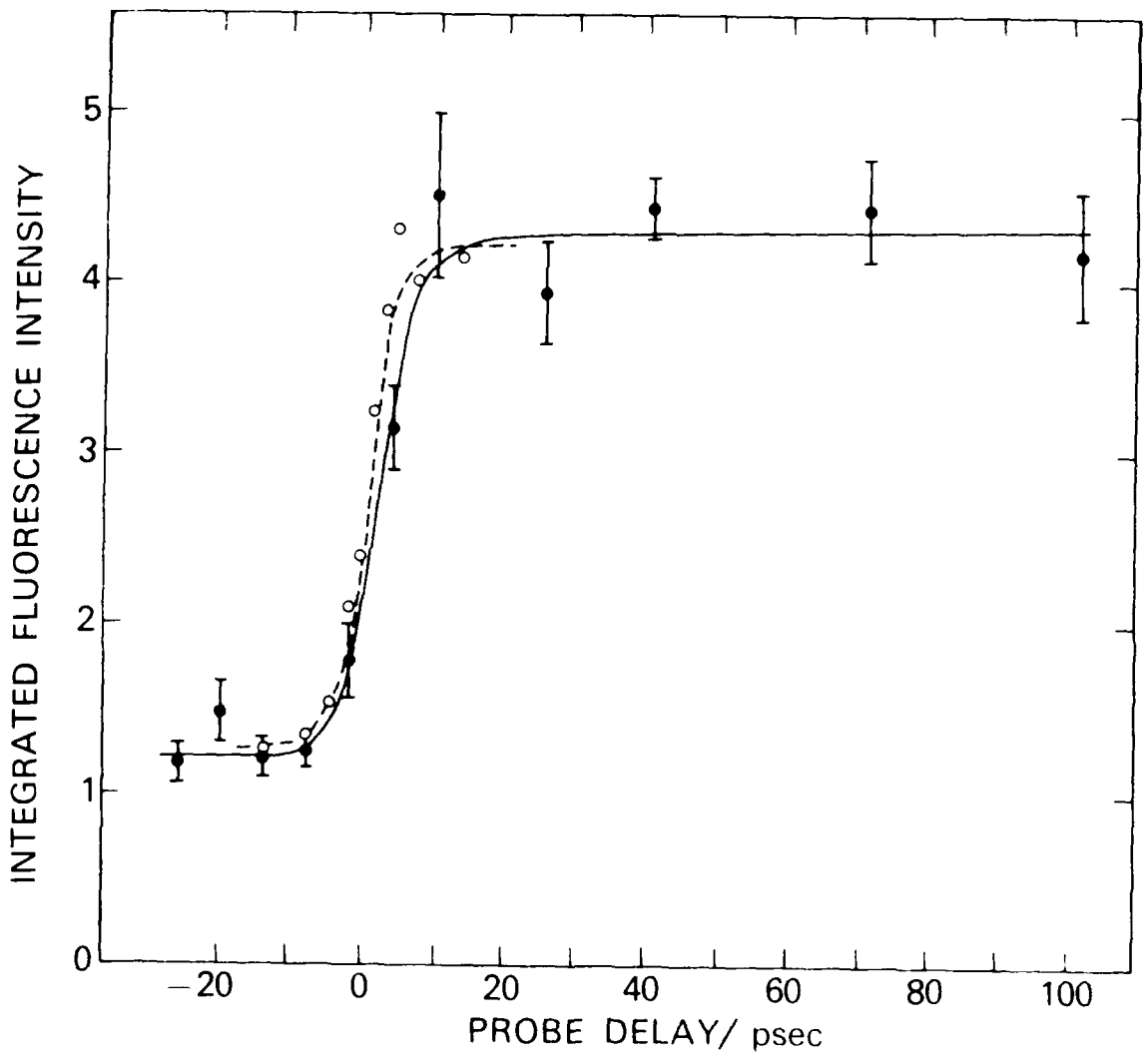

Fig. 1 - Fluorescence from photolyzed nitromethane at a pressure of [illegible] Torr. Lower trace shows emission resulting from a single 5 psec pulse of [illegible] nm light; upper trace shows emission produced by UV irradiation followed after a 200 psec delay by a 527 nm probe pulse. Emission is filtered in both cases with a Corning 2-73 filter which transmits wavelengths > 400 nm.

the pressure range of our experiment, indicating the collision-free lifetime of the emitting species is long. This is qualitatively consistent with the known quenching behavior of NO_2 in various gases [15].

Although the fluorescence signal intensity was too weak to yield a spectrum, use of a sequence of long-wavelength-pass filters indicated that in the region from the probe wavelength to ~ 750 nm the probe-induced emission was broad and featureless. No significant emission signal was observed on the antistokes side of the probe wavelength. Thus the spectral characteristics and long lifetime of the emitting species are clearly consistent with NO_2.

We performed a series of experiments to determine the power-law dependence of the fluorescence. Fig. 2 shows a log-log plot of the time-integrated fluorescence intensity as a function of UV pulse energy, for individual laser shots. The lower curve shows the UV + probe induced fluorescence, normalized by probe pulse energy. The upper curve shows UV-only induced fluorescence. Both curves exhibit a unit slope extending over almost 2 decades in UV energy, indicating an effect linear in excitation pulse energy. Since the energy of the photolyzing photon is ~ 4.7 ev and C-N bond cleavage requires ~ 2.6 ev [17], the excess energy for single UV photon induced photolysis should yield fluorescence only at wavelengths longer than ~ 571 nm. This agrees with our observations.

A variable time delay was introduced between the UV and probe pulses to determine whether there was a measurable induction period between excitation of the nitromethane molecules and the appearance of NO_2 fragments. The results shown in Fig. 3 indicate that the population of ground state NO_2 probed by the 527 nm pulse appears and rises to a plateau within the ~ 4 psec pulse resolution of the experiment. For delay times out to 1 nsec the height of the plateau remains approximately constant. Quantitative results are affected by changes in nitromethane pressure. Each point in Fig. 3 represe-

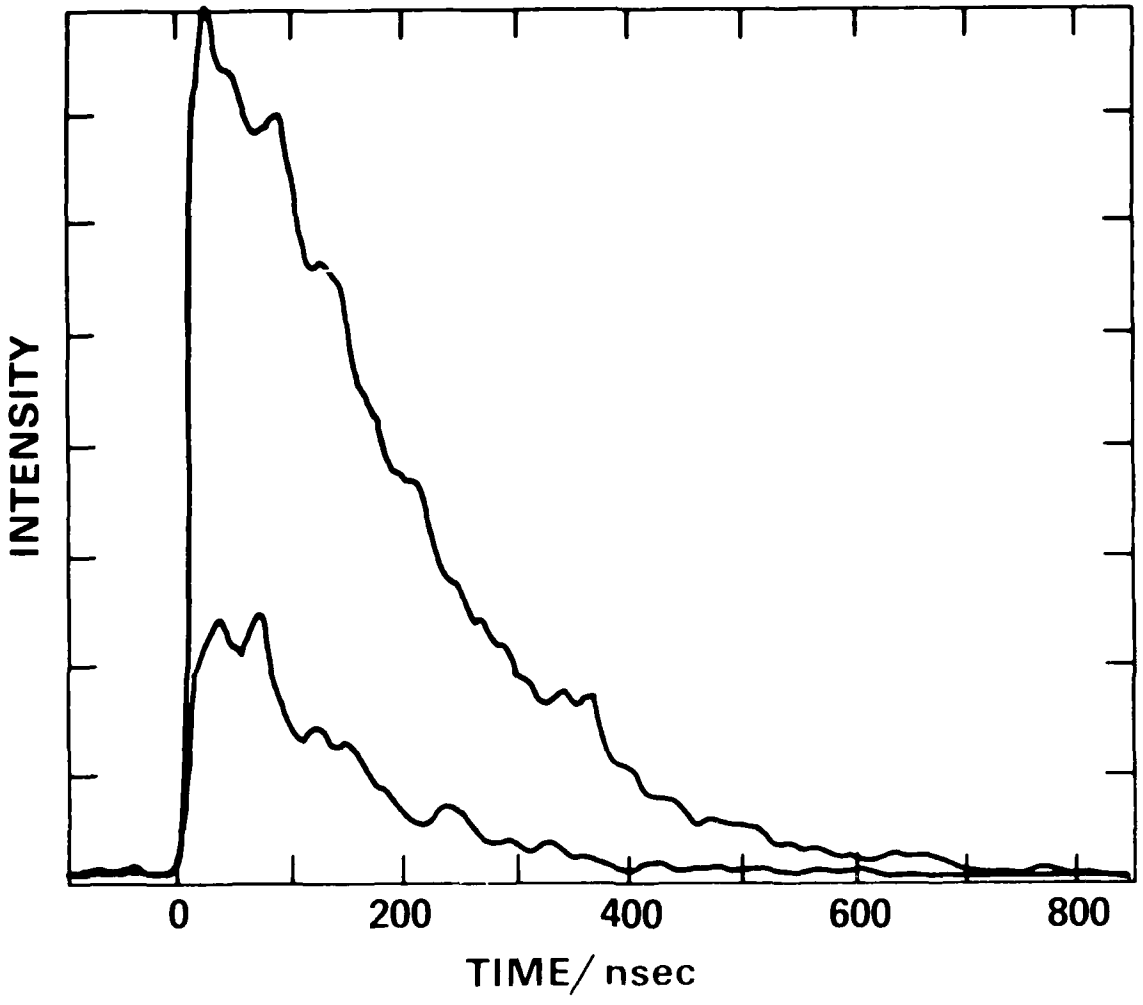

Fig. 2 - Fluorescence power-law dependence in nitromethane photolysis: time-integrated fluorescence signal versus UV excitation pulse energy. Upper trace: Fluorescence caused by UV-only excitation. Lower trace: Fluorescence caused by UV + probe irradiation, normalized to probe pulse energy. Probe time delay was 1 nsec. Nitromethane pressure was 0.2 torr.

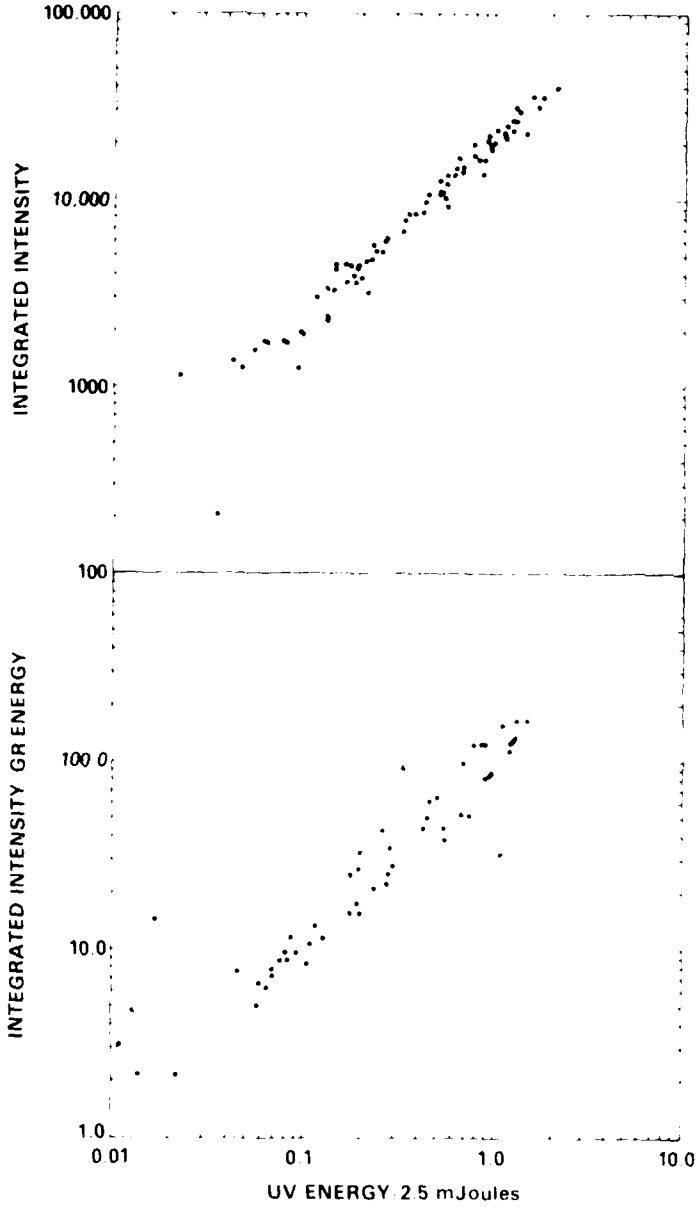

Fig. 3 - Solid line: III signal as a function of probe time delay for nitromethane at 0.8 Torr. Intensity is normalized to UV and probe pulse energies. Each data point represents an average of 10 laser shots. Dashed line: estimated temporal response function (see text) determined by photobleaching experiment in rhodamine dye solution.

sents the time-integrated fluorescence intensity averaged over ten laser shots and normalized to the UV and probe pulse energies. The non-zero fluorescence signal for negative delay times represents the effect of the UV pulse alone.

We have estimated the quantum yield for formation of NO_2 in our experiment to be on the order of 1%. This is the equivalent of ~1 μTorr of NO_2 produced in the laser beam. The calculation assumes unity quantum efficiency for fluorescent re-emission of absorbed 527 nm quanta by unquenched NO_2. Only about 1% of the excited NO_2 molecules radiate before they are collisionally quenched at these pressures of nitromethane.

Discussion

In most early photolysis experiments on nitromethane the final products were determined by chemical analysis, in which case a large number of secondary products were found, including CH_3ONO, CH_2O, CH_3NO, NO, and N_2O [4,6,12]. This, and the dependence of the relative quantum yield of methyl nitrate [2] upon the exciting UV wavelength led to the suggestion that there are other primary photolysis processes besides (I), specifically: [6]

$$CH_3NO_2 \xrightarrow{h\nu} CH_2{=}N{-}\overset{O}{\underset{OH}{}} \rightarrow CH_2O + NOH \qquad (II)$$

and

$$CH_3NO_2 \xrightarrow{h\nu} CH_3NO + O \qquad (III)$$

Rebbert and Slagg [2] suggested that more than one excited state of nitromethane was involved in its decomposition, and Honda et al. [6] and Flicker et al. [18] have supported this idea.

Three excited states of nitromethane have been experimentally identified and connected with its photolysis. Two are observed in the optical absorption spectrum [18-20]: a strong feature at ~190 nm assigned to a $\pi \rightarrow \pi^*$ transition, and a weak satellite at ~260 nm suggested to be an $n \rightarrow \pi^*$, singlet-

singlet excitation. A third, still lower energy state has been found by electron energy-loss spectroscopy [18] at ~ 326 nm, which the authors suggest has $n \rightarrow \pi^*$, singlet-triplet character, but which may be a composite of overlapping transitions of different character. Theoretical calculations indicate that other transitions may exist in this energy region [21-24], but they have not been identified experimentally.

Most investigators have supported process (I) as the main primary photolysis channel for nitromethane [1-5]. Flicker et al. [18] and Honda et al. [6] suggest that the lower energy transition to the triplet state at ~ 326 nm addresses process (I) particularly while the singlet-singlet excitation near 260 nm induces reaction (II).

Both the experiment of Spears and Brugge [8] and our experiment used photolyzing wavelengths in the vicinity of the 260 nm transition and both observed the formation of some NO_2. However, considering the low quantum yield estimated for NO_2 formation in our experiment, the possibility of other decay channels cannot be excluded.

Summary

We have studied photolysis of nitromethane gas at pressures of $\leq$ 3 Torr. The photolyzing 264 nm pulse itself produces some NO_2 in an excited fluorescing state. Laser-induced-fluorescence probing using a time delayed second-harmonic pulse reveals formation of a ground state NO_2 population in ~ 5 psec, which remains roughly constant for probe delay times extending to 20 ns. An estimate of quantum yield for the photodecomposition appears to be rather low (~ 1%) at this photolyzing wavelength.

The observed fluorescence intensity scales linearly with UV pulse energy. The LIF signal which monitors ground state NO_2 is also linear in both UV and probe pulse energies.

Acknowledgments:

The authors wish to thank Prof. R. G. Weiss for his very useful advice and discussions. We also gratefully acknowledge the Office of Naval Research Power Program for partial support of this research.

References

1. E. Hirschlaff and R. G. W. Norrish, J. Chem. Soc. 1580 (1936).

2. R. E. Rebbert and N. Slagg, Bull. Soes. Chim. Belges. 71, 709 (1962).

3. B. H. J. Bielski and R. B. Timmons, J. Phys. Chem. 68, 347 (1964).

4. I. M. Napier and R. G. W. Norrish, Proc. Roy. Soc. A299, 317, (1967).

5. R. B. Cundall, A. W. Locke and [illegible] C. Street, in "The Chemistry of Ionization and Excitation," [illegible] R. A. [illegible]ssen and [illegible] Scholes, eds. (Taylor Francis, Ltd., London, 1967) [illegible].

6. K. Honda, H. Mikuni [illegible] M. [illegible]earist, Bull. Chem. Soc. Jpn. [illegible], 353, (1972).

7. M. J. Collins, A. M. Ancus, E. F. Marmarr, Nature, [illegible], 881 (19[illegible]).

8. K. G. Spears and S. P. Bragg [illegible], Chem. Phys. Lett. 52, 3 3 (197[illegible]).

9. V. [illegible] Frist, L. S. Goldberg, F. R. Royt, J. N. Bradford, [illegible]. M. Sharp, P. [illegible] Stock and S. G. Weiss, in "Photoelectron Spectroscopy," [illegible]. W. Shirley, D. A. Lipper and B. J. Snapir, eds. Interscience, N.Y. (197[illegible]), p. 23.

10. Ph. Avouris, J. Y. Chan and M. A. [illegible], J. Photochem. 12, 33 (1980).

11. B. H. Rockey and [illegible]. R. Grant, Chem. Phys. Lett. [illegible], 1 (1[illegible]).

12. H. S. Kwok, J. [illegible] Ho, R. K. Sparks and Y. [illegible] Lee, [illegible] Int. J. Chem. Kinetics.

13. L. S. [illegible]lberg, P. E. Schoen and [illegible]. [illegible] Chem. Phys. [illegible].

14. L. F. Keyser, S. [illegible] Leone and [illegible]. Stief, J. Chem. Phys. [illegible], 3[illegible] (1971).

15. V. M. Donnelly, D. G. Keil and [illegible] Kaufman, J. Chem. Phys. [illegible], 959 (19[illegible]).

16. R. W. B. [illegible]arre and A. J. Gordon, "The [illegible]ntification of Molecular Spectra," (Chapman and Hall, London, 19[illegible]).

17. R. Kandel, J. Chem. Phys. 23, 84 (1[illegible]).

18. W. M. Flicker, O. A. Mosher and [illegible]. Kuppermann, Chem. Phys. Lett. [illegible], 418 (1979).

19. S. D. Taylor, T. D. Allston, M. [illegible] Moscat[illegible], G. B. [illegible]nakos, R. Kozlowski, and G. A. Takacs, Int. J. of Chem. Kinetics, 12, 231 (198[illegible]).

20. S. Nagakura, Mol. Phys. 3, [illegible] (196[illegible]).

21. J. W. Rabalais, J. Chem. Phys. 57, 960 (1972).

22. G. E. Harris, J. Chem. Phys. 58, 5615 (1973).

23. J. N. Murrell, S. Al-Dabi and S. F. Guest, J. Chem. Soc. Faraday Trans., II 71, 1577 (1975).

24. K. L. McEwen, J. Chem. Phys. 32, 1537 (1960).

HIGH POWER PICOSECOND PHOTOLYSIS OF SIMPLE ORGANIC MOLECULAR GASES*

P.B. Craig**, W.L. Faust, L.S. Goldberg, L.M. Schnur, P.F. Schoen, and R.G. Weiss**

Naval Research Laboratory, Washington, DC 20375 U.S.A.
**Department of Chemistry, Georgetown University, Washington, DC 20057 U.S.A.

ABSTRACT

High power picosecond ultraviolet pulses from a Nd:YAG modelocked laser were used to induce a visible emission from a variety of gaseous organic molecules. We report the observation of electronically excited C$_2$, CH, CN, and H fragments. The spectral characteristics and time development of the emitting species are highly dependent upon the structure of the parent molecules.

INTRODUCTION

Laser photolysis of simple molecules has contributed to a deeper understanding of dynamical processes in photodissociation. Our concern in the present work is with the decomposition of simple compounds which afford generic models of processes important in explosives, fuels, and other energetic materials. Multiphoton IR and UV laser dissociation (1-4) have previously been applied to study the primary decomposition processes of gas-phase molecules and subsequent reaction of fragments having significance to the kinetics of combustion. These experiments have been performed in the nanosecond time domain and at millitorr gas pressures in order to maintain a collision-free time regime

* This work supported in part by the Office of Naval Research and the Strategic Defense Initiative Organization.

during the duration of the excitation pulse. In our experiments the time resolution afforded by picosecond pulse excitation enables such photolysis even at atmospheric pressures, yielding high fragment concentrations. For the pressures and high flux densities employed in this work, multiphoton absorption processes can be accompanied by dielectric breakdown (5). Indeed, since laser-induced breakdown is a nonresonant process, this very nonspecificity facilitates the decomposition of a wide variety of materials.

Here, we demonstrate the utility of the technique in generating fragments whose emission spectra reflect their precursors. We have carried out the photolysis of benzene, methane, carbon dioxide, and nitromethane at pressures in the range of 1–500 torr, and studied the luminescence from C_2, CH, CN, and H fragments.

EXPERIMENTAL

Figure 1 shows a schematic of the Nd:YAG laser system. The flashlamp-pumped oscillator, operating at a 1 Hz repetition rate, employed a hybrid modelocking approach to provide more reproducible pulse-train generation.

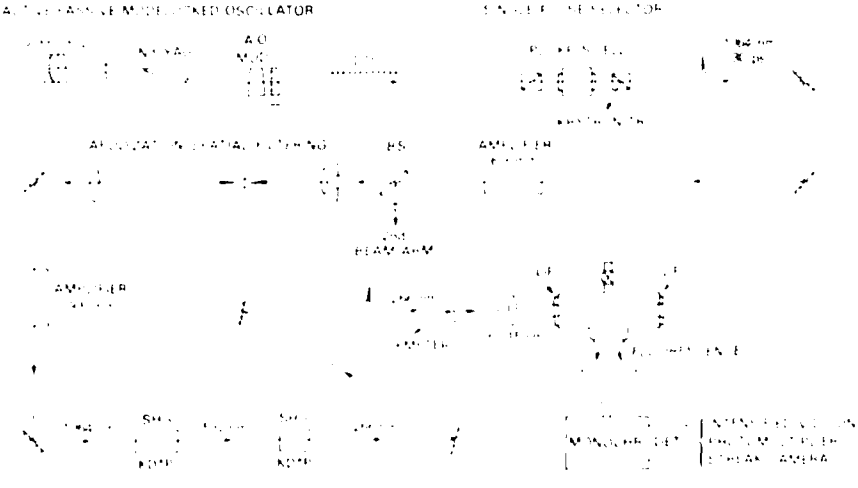

Figure 1. Schematic of the laser system.

It utilized an active acousto-optic loss modulator (Quantronix) and a passive saturable absorbing dye (Eastman A9740) in a flow cell. The single 1064 nm pulse, switched from near the peak of the train, had ca. 0.4 mJ energy and typically 30 ps duration. Two stages of amplification, apodization, and spatial filtering of the beam provided a high-spatial-quality IR pulse of 3-4 mJ energy. Efficient frequency doubling and mixing in KD*P crystals generated a 4th harmonic (266 nm) photolysing pulse of up to 10 mJ energy. The laser beam was focused to a 0.1 mm diameter in a static gas cell (ca. 100 cm³) through a CaF window. The emitted light generated from individual laser shots was collected at right angles and focused into a scanning monochromator coupled to a Nuclear Data ND100 intensified diode multi-channel recording system (spectral sensitivity 300-800 nm). Improved signal-to-noise was achieved where necessary by accumulating data from typically 30 laser shots. High-resolution spectra were obtained with a Spex 0.8 m monochromator (0.1 nm system resolution). For time-resolved studies, a Varian VPM-159M crossed-field photomultiplier was coupled to the exit slit of the monochromator. The transient signal was displayed on a Tektronix 7104 oscilloscope, giving a detection risetime of 400 ps. Observations were also made with an Electrophotonics streak camera (S-20 photocathode) having time resolution of 10 ps.

Methane was research grade purity supplied by Matheson Gas Products and was used without further purification. Carbon monoxide was ultra-high purity grade (Matheson) and was freed of any metal carbonyl contaminants by passing through a heated tube (200°C, atmospheric pressure) packed with glass wool (6). Nitromethane was Baker reagent grade and was distilled under nitrogen, collecting the middle fraction, b.p. 101-102°C. Ketene, CH_2CO was prepared by a standard procedure (7) involving dehydration of acetic anhydride at 500-550°C and was purified by trap-to-trap distillation. It was stored in the dark under vacuum in a liquid nitrogen bath. A salt-ice bath placed between the reservoir and the sample cell was used to condense traces of acetic acid and other high-boiling impurities.

RESULTS AND DISCUSSION

High power, 30 ps pulses at 266 nm focused into the vapors under study (10-500 torr) generated a visible streak near the focal region. Low- and high-resolution spectra of the luminescence exhibited no differences in intensity or spectral distribution during a typical experiment involving several hundred laser shots. This indicates that stable photolytic products do not significantly affect the primary decomposition processes. The result is not surprising since the photolysed region is at least 10^6 smaller than the total sample volume. It should be emphasized that our analytical techniques give evidence only of luminescent species; other intermediates are undoubtedly produced.

Figure 2 depicts the similarity of the low-resolution emission spectra from ketene and carbon monoxide, each at 100 torr. High resolution spectra indicate that the predominant emission belongs to the C_2 diradical in its triplet $d^3\Pi_g \rightarrow a^3\Pi_u$ Swan transition (8).

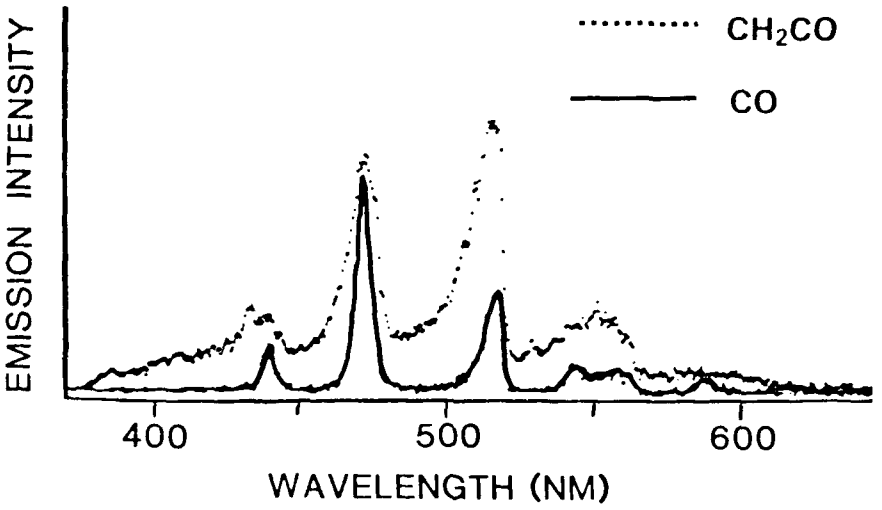

Figure 2. Low-resolution (2 nm) emission spectra obtained when ketene and carbon monoxide, at 100 torr, are irradiated with individual laser pulses at 266 nm.

Figures 3 and 4 show the $\Delta v = 0$ and $\Delta v = -1$ transitions for C_2 from carbon monoxide, methane, and ketene. The emission spectra from methane and ketene exhibit a strong attendant rotational structure. In addition, a weak, underlying continuum emission, associated with a plasma formation, extended throughout the visible region. The intensity of this background varied for each gas studied but was most prominent for methane. Figures 5 and 6 compare the regions of Swan $\Delta v = +1$ and $\Delta v = +2$ emission from carbon monoxide and ketene. Striking dissimilarities are evident at this resolution. Only in the case of CO are the C_2 "high-pressure" bands (9) observed. These are a consequence of the selective population of an upper vibrational level (generally attributed to $v' = 6$) (9) of the $d^3\Pi_g$ state and necessitate distinct formation mechanisms for the C_2 produced from carbon monoxide and ketene.

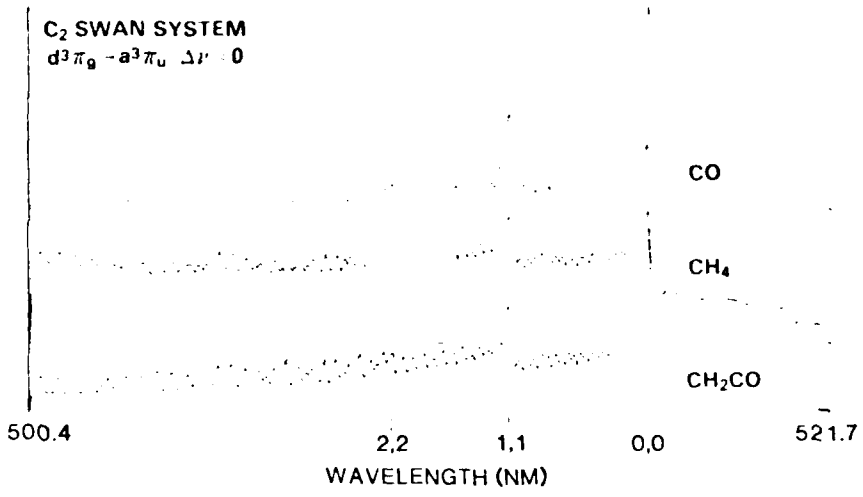

Figure 3. High-resolution (0.1 nm) spectra of the Swan system emission ($\Delta v = 0$) derived from 266 nm irradiation of carbon monoxide, methane, and ketene, at 100 torr. Data are accumulated from 30 laser shots. Note the strong rotational decoration, to the high-energy side of the band heads, for methane and ketene.

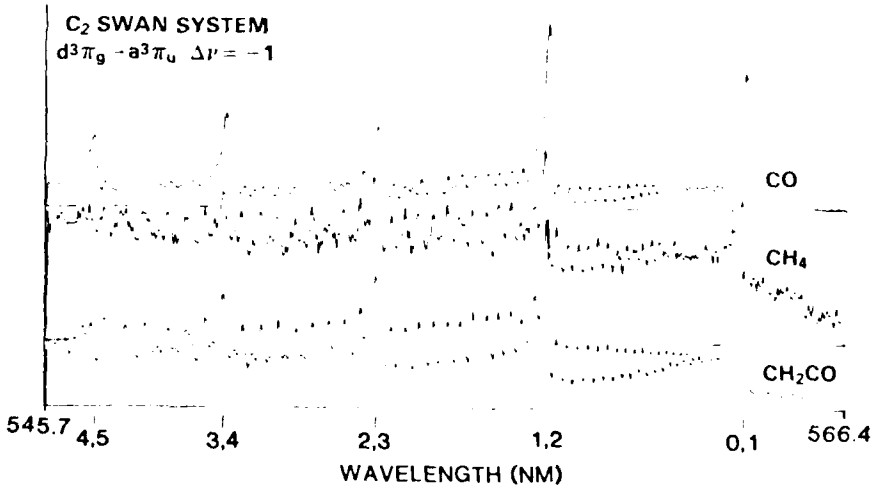

Figure 4. Spectra of the Swan system emission ($\Delta v = -1$). Conditions as in Figure 3.

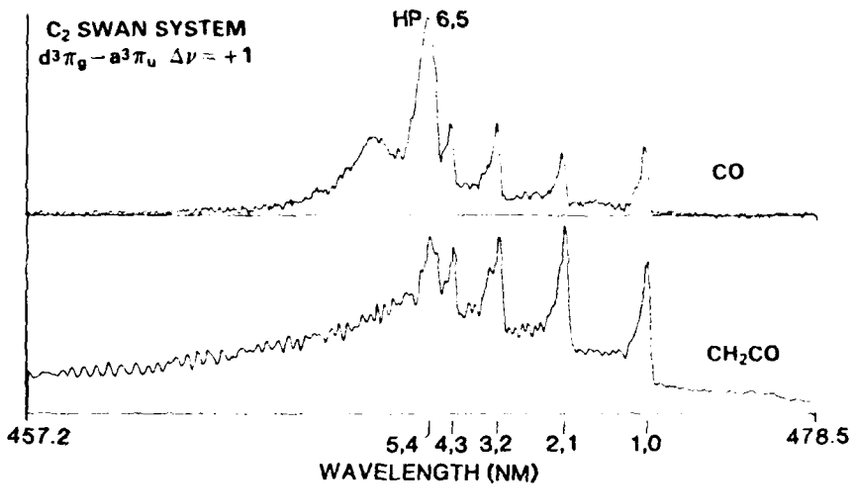

Figure 5. Spectra of the Swan system emission (Δv = +1) derived from carbon monoxide and ketene, at 100 torr. Data are accumulated from 30 laser shots. The spectrum from CO also shows the high-pressure 6,5 band.

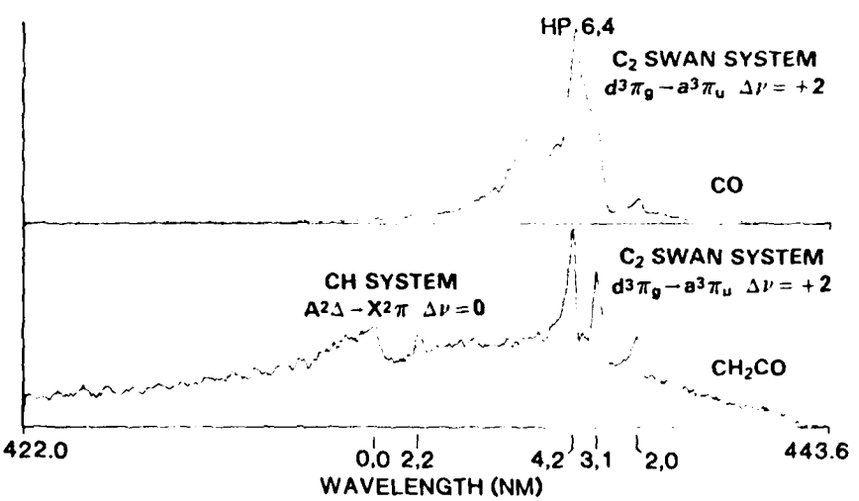

Figure 6. Spectra of the Swan system emission (Δv = +2). Conditions as in Figure 5. The spectra also show the high-pressure 6,4 band and CH emissions.

This difference of mechanisms finds further expression in the time-dependent oscilloscope data shown in Figure 7.

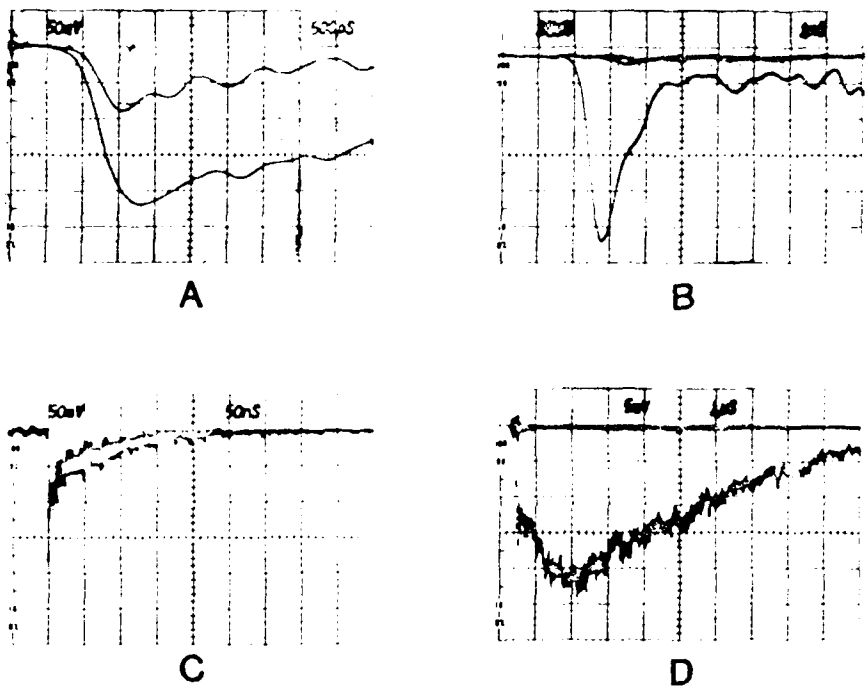

Figure 7. Oscilloscope traces of the C_2 Swan emission monitored at 516 nm ($0,0$ transition). A: ketene, 200 torr, 500 μs/div. The upper trace shows the plasma radiation at 516 nm. B: CO_2, 100 torr, 1 ns/div. C: ketene, 400 torr, 50 ns/div. D: CO_2, 100 torr, 1 μs/div.

Figure 7A shows the risetime-limited formation of the $d^3\Pi_g$ emissive state (at 516 nm) of C_2 derived from ketene. The risetime is indistinguishable from that of the plasma radiation

(upper trace), monitored at 616 nm where Swan emission is negligible. By contrast, no prompt C_2 emission is seen from CO (Fig. 7B) when either the normal or the high-pressure Swan bands are monitored. The oscillogram in Figure 7B shows only the brief plasma emission, which can be detected throughout the visible region. Over much longer timescales (Fig. 7D), the slow, collisional formation of the $d^3\Pi_g$ state is observed. An intermolecular pathway leading to the formation of C_2, like that suggested by Kopp et al. (10) (Eq. 1 and 2), is consistent with these data:

$$C + CO + M \rightarrow C_2O + M \quad (1)$$

$$C_2O + C \rightarrow C_2^* + CO \quad (2)$$

M represents a third body and * refers to an unspecified electronic state of C_2. The highly-specific vibrational population of the excited state is then rationalized as follows: there is a relaxation of the initial C_2 state to $b^3\Sigma_g^-$ which crosses $d^3\Pi_g$ near its sixth vibrational level (11). It has generally been accepted that the high-pressure emission originates from $v' = 6$. However, the high-pressure bands lie to the low energy side of the corresponding normal Swan band head, where there are no rotational term differences. For example, the designated 6,5 high-pressure transition is at 468.0 nm while the regular 1,0 Swan band is observed at 466.9 nm (8,12). On this basis, we infer that the exact crossing between the $b^3\Sigma_g^-$ must occur below $v' = 6$.

Since the $d^3\Pi_g$ state collision-free lifetime has been determined as ca. 120 ns (3), it is clear that the slower decay in Figure 7D does not reflect the kinetics of the $d^3\Pi_g \rightarrow a^3\Pi_u$ transition. Evidently we are following the formation and decay steps of an intermediate (consistent with Equation 1 and 2), which become the rate-determining processes for the C_2 $d^3\Pi_g$ emission. Figure 7C indicates that the C_2 $d^3\Pi_g$ state has a lifetime of ca. 7 ns, when produced in 100 torr of ketene. It is likely that the parent molecule and/or other photolysis fragments are involved in quenching steps. For instance, all the hydrogen bearing gases exhibit a strong pressure-broadened emission line at 656.3 nm, assigned to the Balmer $H\alpha$ line of atomic hydrogen (Fig. 8).

Returning to Figure 7A, the C_2 derived from ketene appears with detection-system risetime (the contribution of the plasma to the lower trace is limited). Such prompt C_2 formation suggests a unimolecular mechanism. However, a rapid collisional formation may be envisaged if the reacting fragments are created with substantial kinetic energy. Attempts to observe the formation using a streak camera have proved inconclusive. The spectral resolution required to minimize the prompt background has not allowed sufficient signal to be detected from the C_2 emission. In

the case of methane, where C_2 production must be a collisional process, we have nonetheless been unable to follow it kinetically. The plasma radiation dominates the transient signal at 100 torr of methane for several nanoseconds, by which time the C_2 signal is fully developed.

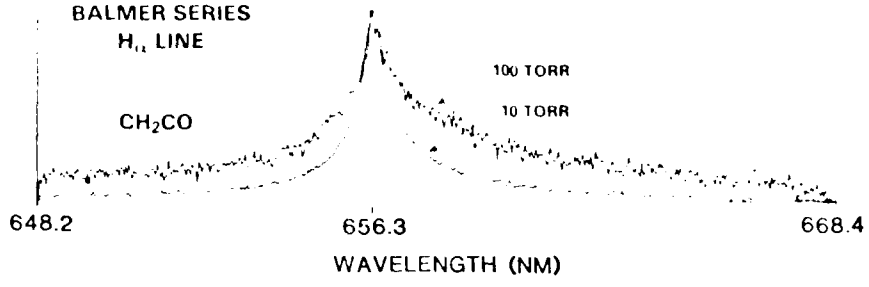

Figure 8. Spectra of the atomic hydrogen Hα emission line derived from 266 nm irradiation of ketene. Note the strong pressure-broadening effect.

The C_2 emission from methane and ketene show considerable rotational excitiation, which implies a non-thermally-equilibrated population of excited C_2 molecules. C_2 emission spectra showing such abnormal rotation are ubiquitous in discharge (13) and laser photolysis (3) studies of simple organic molecules. In an intermolecular mechanism, "*off-axis*" collisions between fragments would be expected to impart excess rotation to a C_2 product. It is also possible that ketene undergoes unimolecular elimination of hydrogen and oxygen via out-of-plane bending motions, leaving C_2 with rotation. In the case of CO, the C_2 high-pressure system is obtained together with the normal Swan system, both showing the same protracted time development. This now gives temporal as well as spectral inference that C_2 is formed from CO by processes entirely distinct from those in ketene and methane. Consequently, it is not surprising that the emission spectrum exhibits much less rotational fine structure than that derived from ketene and methane.

Weak lines were observed at 410.2 nm and 406.8 nm only when ketene was photolysed. They are attributed to the Deslandres-d'Azambuja singlet C_2 system ($C^1\Pi_g \rightarrow A^1\Pi_u$, $\Delta v = -1$) (8). A weak fluorescence at 431.4 nm (Fig. 6), observed for ketene and methane is attributed to CH emission ($A^2\Delta \rightarrow X^2\Pi$, $\Delta v = 0$) (8).

The power dependence of the C_2 emission is displayed in Figure 9. At high input pulse energies, both carbon monoxide and ketene (100 torr) show a near-linear power dependence indicative

of a saturation regime. The high-order nature of the excitation process is clearly evident from the steepening of the curves towards lower input energies. Furthermore, focusing of the excitation beam was essential for producing observable emission. Carbon monoxide and methane showed no emission at pressures below 10 torr. Ketene, however, which possesses a single-photon transition at 266 nm ($\varepsilon \sim 0.5$ mol^{-1} cm^{-1}) (14), exhibited luminescence even at pressures below 1 torr. The streak of visible emission extended somewhat beyond the focal region and had a more diffuse appearance than that observed at higher pressures. The excitation processes may well be different at lower pressures, but the observed luminescent products appear the same.

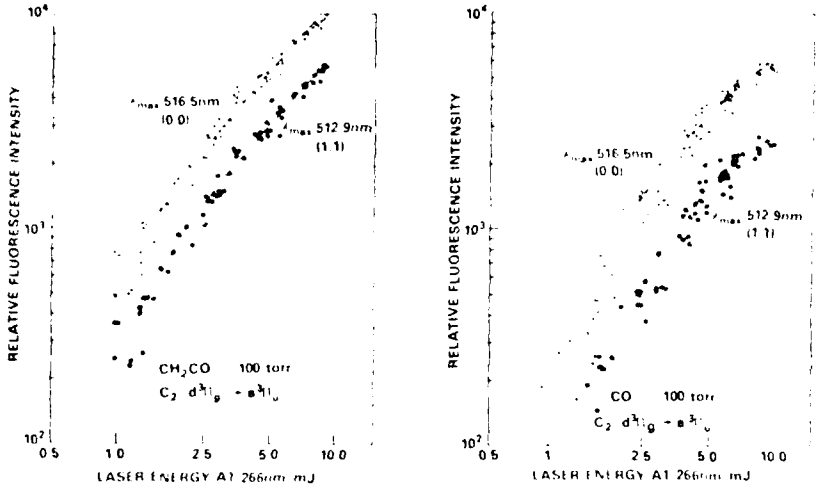

Figure 9. Dependence of the C_2 Swan emission intensity on input laser pulse energy at 266 nm, from ketene (left) and carbon monoxide (right), at 100 torr.

Figure 10 compares the $\Delta v = 0$ C_2 Swan system observed from 15 torr of nitromethane with that from 10 torr of ketene. The C_2 band is substantially weaker in the case of nitromethane. It shows excess rotational excitation, as for ketene and methane. Furthermore, two new strong emissions were observed with band heads at 421.6 nm and 388.3 nm (Fig. 10, below). These are assigned to the violet system of CN and arise from $B^2\Sigma^+ \rightarrow X^2\Sigma^+$ transitions (8). The $\Delta v = 0$ transition was also weakly observed in the case of ketene and carbon monoxide, indicating a slight nitrogen impurity.

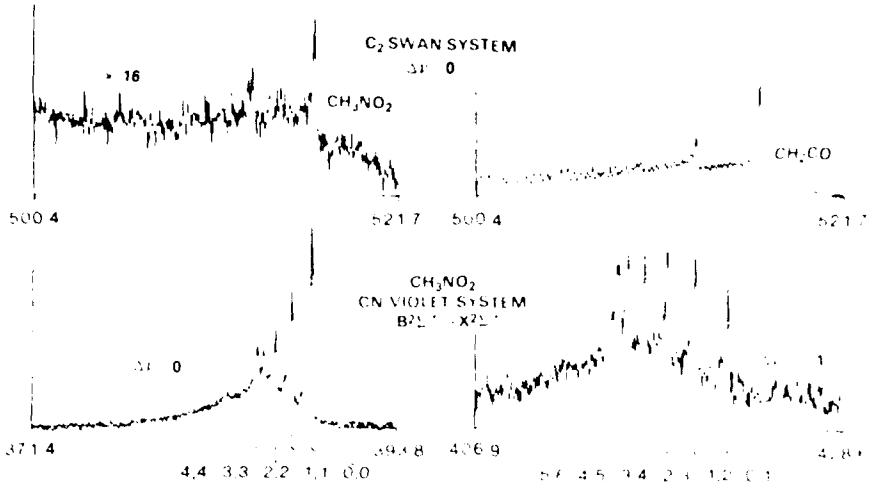

Figure 10. Above: Spectra of the C$_2$ Swan emission ($\Delta v = 0$) derived from ketene at 10 torr and nitroethane at 15 torr. Note the reduced intensity of the signal from nitroethane. Below: Spectra of the CN violet system emission ($\Delta v = 0$, $\Delta v = -1$) derived from nitroethane at 15 torr. Data are accumulated from 30 laser shots.

The appearance of the strong CN emission from nitroethane and corresponding decrease in the C$_2$ emission might indicate that even under these harsh excitation conditions, the C-N bond remains intact. On the other hand, observations from conventional photolysis have been interpreted to support scission of the C-N bond as the main primary process (15). The CN fragment from nitroethane could be generated unimolecularly, whereas by necessity C$_2$ is produced collisionally. Experiments are now in progress to follow the time development of the CN emission. In addition, we are examining other nitroalkane alkanes which could provide an intramolecular C$_2$ formation pathway as a competing process with CN production.

SUMMARY

In this work we have extended to the picosecond regime the time definition for laser initiation and interrogation of gas-phase molecular dissociation, with spectral resolution adequate to isolate individual fragment species and indeed to observe

rotational structure. We have examined the spectral and temporal characteristics of the dominant emitting transients, C_2, CH, CN, and H, observed in intense picosecond UV irradiation of ketene, methane, carbon monoxide, and nitromethane. The rapid production of the C_2 $d^3\pi_g$ state from methane and ketene (limited by the detection system risetime) suggests a similar mechanism of collisional formation, although a unimolecular process can not be ruled out in the case of ketene. Pyrolysis of CO also yields the C_2 $d^3\pi_g$ state, which develops and decays collisionally over several microseconds. Its spectrum exhibits the $\Delta v = 2$ sequence bands and shows much less rotational excitation than that obtained from ketene and methane. It is [illegible] vibrationally unthermalized C_2 $d^3\pi_g$ [illegible] are V_2 correlated from precursors bearing CH_x. For [illegible], this [illegible] studies of the weak C_2 signal and [illegible] could also provide some insight into the [illegible] Future application of this technique to the [illegible] and other related compounds may provide [illegible] for [illegible] transitions through which these [illegible] participate in the early stages of rapid decomposition.

REFERENCES

1. Ambartzumian, R.V., Chekalin, S.V., [illegible], V.S., and Ryabov, V.A.: 1975, Chem. Phys. Lett. 36, pp. [illegible].

2. Jesiński, M.L., and Grillory, W.A.: 1977, J. Chem. Phys. 66, pp. 4315-4324.

3. McDonald, J.R., Baronavski, A.P., and Donnelly, V.M.: 1978, Chem. Phys. 33, pp. 161-170.

4. Filseth, S.V., Hancock, G., Kornier, J., and Meier, K.: 1979, Chem. Phys. Lett. 61, pp. 288-292.

5. Konn, A.M.: 1976, Chem. Phys. Lett. 42, pp. [illegible].

6. Braker, W., and Mossman, A.L.: 1971, "Matheson Gas Data Book."

7. Sutall, R.L., Lauter, A.H., and Kilday, M.V.: 1971, J. Chem. Thermodyn. 3, pp. 167-174.

8. Pearse, R.W.B., and Gaydon, A.G.: 1965, "Identification of Molecular Spectra," Chapman and Hall, London.

9. Herzberg, G.: 1946, Phys. Rev. 70, pp. 762-764.

10. Kunz, C., Harteck, P., and Dondes, S.: 1967, J. Chem. Phys. 46, pp. 4157-4158.

11. Read, S.M., and Vanderslice, J.T.: 1962, J. Chem. Phys. 36, pp. 2366-2369.

12. Johnson, R.C.: 1927, Phil. Trans. Royal Soc. A 266, pp. 157-230.

13. Lochte-Holtgreven, W.: 1930, Z. für Physik. 64, pp. 443-451.

14. Laufer, A.H., and Keller, R.A.: 1971, J. Am. Chem. Soc. 93, pp. 61-63.

15. Honda, K., Mikuni, H., and Takahasi, M.: 1972, Bull. Chem. Soc. Japan, 45, pp. 3534-3541.

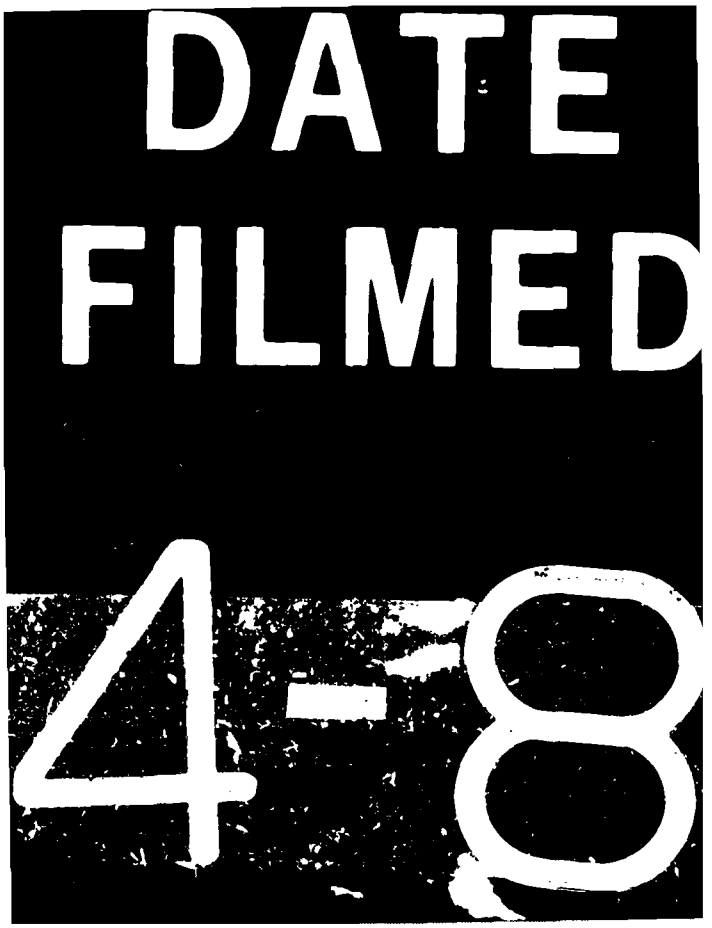
DATE
FILMED
4-8